

# **Design and Development of Load Motor for Vector Control**

*A Project Report*

*submitted by*

**AMAYA S DHOBLEY**

*in partial fulfilment of the requirements  
for the award of the degree of*

**MASTER OF TECHNOLOGY**



**DEPARTMENT OF Electrical Engineering  
INDIAN INSTITUTE OF TECHNOLOGY MADRAS.**

**15th June,2020**

# THESIS CERTIFICATE

This is to certify that the thesis titled **Design and Development of Load Motor for Vector Control**, submitted by **Amaya S Dhobley**, to the Indian Institute of Technology, Madras, for the award of the degree of **Master of Technology**, is a bona fide record of the research work done by him under our supervision. The contents of this thesis, in full or in parts, have not been submitted to any other Institute or University for the award of any degree or diploma.

**Dr.Kamalesh Hatua**

Research Guide

Professor

Dept. of Electrical Engineering

IIT-Madras, 600 036

Place: Chennai

Date: 15 June 2020

## ACKNOWLEDGEMENTS

I would like to express my special thanks of gratitude to my guide **Dr.Kamalesh Hatua** for give me such an wonderful opportunity to learn and work on this project.I consider myself extremely fortunate to have worked under his guidance.Despite of his busy schedule the support he provided support and constant piece of advice with full of encouragement thoughts.I will also like to thank him for providing Laboratory facility in the Electrical Machines Laboratory,Department of Electrical Engineering ,IIT Madras.

I consider myself fortunate enough to have attended lectures delivered by Dr.Lakshminarsamma which helped me in developing my interest towards Power electronics and Drives field.

I would also like to thank my Laboratory colleagues and Batch mates(Batch-2020,Mtech) for helping me out and constantly providing support naming them Srikrishnan,Harikrishnan,Jose,Himanshu.

Lastly i would like to thank my family members who kept faith in me and had my back during hard times.

# **ABSTRACT**

**KEYWORDS:** Vector Control, Online Modeling

Vector control of Induction motor is very highly efficient motor control technique which gives dynamic performance almost similar to Dc motor drive which has excellent dynamic torque response and speed response. In this method all the machine variables are transformed into rotor flux frame, so that Induction motor can be modeled and controlled similar to DC machine. This scheme intends to independently control Torque generating vector and flux producing vector with the prior knowledge of rotor flux position .

In this Project work MATLAB Simulation for Voltage speed control of Separately Excited DC motor and Vector Control of Induction motor , Online modeling of Induction motor , V/f control of Induction motor is carried out on TMS320F28379D DSP Launchpad from Texas Instruments. DC motor is rated for 10HP while Induction motor is rated for 30KW.

# TABLE OF CONTENTS

<b>ACKNOWLEDGEMENTS</b>	<b>i</b>
<b>ABSTRACT</b>	<b>ii</b>
<b>LIST OF FIGURES</b>	<b>vi</b>
<b>ABBREVIATIONS</b>	<b>vii</b>
<b>NOTATION</b>	<b>viii</b>
<b>1 Separately excited DC motor speed control</b>	<b>1</b>
1.1 Introduction . . . . .	1
1.2 Voltage speed control method . . . . .	2
1.3 Design of steady state model . . . . .	3
1.4 Design of Controllers . . . . .	5
1.4.1 Current Controller . . . . .	5
1.4.2 Speed controller . . . . .	6
1.5 Simulation results . . . . .	8
<b>2 Vector control of Induction motor</b>	<b>11</b>
2.1 Introduction . . . . .	11
2.2 Vector Control . . . . .	11
2.2.1 Clarke's transformation . . . . .	12
2.2.2 Park's transformation . . . . .	13
2.2.3 Power Inverter(VSI) . . . . .	14
2.2.4 Mathematical modeling . . . . .	15
2.2.5 Design of Controllers: . . . . .	23
2.3 Simulation results: . . . . .	28
<b>3 Overview of DSP(TMS32028379D)</b>	<b>31</b>
3.1 Introduction . . . . .	31

3.2	ePWM Module: . . . . .	32
3.2.1	TimeBase Submodule . . . . .	33
3.2.2	Counter-Compare Submodule . . . . .	34
3.2.3	Action Qualifier Sub-module . . . . .	34
3.2.4	Dead Band Generator Sub-module . . . . .	35
3.2.5	Event Trigger Sub-module . . . . .	35
3.3	ADC Module . . . . .	36
3.4	DAC Module: . . . . .	37
3.5	eCAP Module: . . . . .	37
<b>4</b>	<b>DSP simulations</b>	<b>39</b>
4.1	R-L simulation in DSP . . . . .	39
4.1.1	Analytical solution: . . . . .	39
4.1.2	Implementation in DSP . . . . .	39
4.2	Online Modeling of Induction motor . . . . .	41
4.3	V/f applied to Induction motor. . . . .	44
4.4	Vector control implementation . . . . .	47
4.4.1	Per unitized model for IM(30KW) . . . . .	47
4.4.2	controller constants in per unit . . . . .	48
4.4.3	Flux angle estimation . . . . .	49
<b>5</b>	<b>Conclusion</b>	<b>51</b>
5.1	Summary of work . . . . .	51
5.2	Future scope . . . . .	51

## LIST OF FIGURES

1.1	Block diagram for speed control of separately excited DC motor . . .	1
1.2	Torque vs Rotor speed plot for control strategies of separately excited DC motor. . . . .	2
1.3	Current controller loop for separately excited DC motor. . . . .	5
1.4	Speed controller loop for separately excited DC motor . . . . .	7
1.5	Bode plot depicting symmetric optimum pole placement. . . . .	7
1.6	DC motor parameters. . . . .	8
1.7	DC motor speed plot when full load torque is applied at t=1 sec. (Scale: X-axis 2sec/div ,Y-axis 20A/div) . . . . .	9
1.8	DC motor speed profile when supply is given at t=1sec at full load torque,with speed reference of 1400rpm. ( Scale: X-axis 2sec/div ,Y-axis -1000rpm/div.) . . . . .	9
2.1	Block diagram for Vector Control of Induction motor. . . . .	12
2.2	In figure 2.2, Figure 1 represents Clarke's transform and Figure 2 represents Park's transform . . . . .	13
2.3	Phasor diagram for Vector control. . . . .	14
2.4	Equivalent circuit of Induction motor in Space Phasor domain. . . .	16
2.5	Anti-windup PI controller block diagram. . . . .	24
2.6	Figure represents q - axis current controller loop,d-axis current loop will be similar to this. . . . .	25
2.7	Flux controller loop. . . . .	26
2.8	Bode plot for symmetric optimum pole placement. . . . .	26
2.9	Speed controller loop. . . . .	27
2.10	Induction motor 3 phase current profile during starting with vector control.(Scale: X-axis 2 sec/div , Y-axis 100A/div) . . . . .	29
2.11	Speed response with full load torque being applied from starting.(Scale: X-axis 2 sec/div , Y-axis 500 rad/sec /div) . . . . .	29
2.12	d-axis and q-axis current plots for Vector control(Scale: X-axis 2sec/div , Y-axis 50A/div.) . . . . .	30
3.1	Block diagram showing basic features available in TMS320F28379D DSP . . . . .	32

3.2	Block diagram showing features of EPWM module. . . . .	33
3.3	Block diagram showing ADC module. . . . .	36
3.4	eCAP ModuleReference-Technical reference module TI,literature no.SPRUHM8I,December-2013-Revised September 2019. . . . .	38
4.1	RL load simulated in DSP with Orange line as voltage signal and green line as current signal. ( Scale: X-axis 2sec/div , Y-axis 20units/div.)	41
4.2	a phase Rotor current profile for Induction motor at no load. ( Scale: X-axis 5msec/div , Y-axis 500 units/div.) . . . . .	42
4.3	shows Torque profile for Induction motor at no load. ( Scale: X-axis 5msec/div , Y-axis 500rpm/div.)at no load . . . . .	42
4.4	d-axis and q-axis profiles for dq reference currents. Upper one repre- sents Isd,lower one represents Isq ( Scale: X-axis 5msec/div , Y-axis 500mv/div.) . . . . .	43
4.5	sine(rhomr) plot vs supply sine wave. ( Scale: X-axis 5msec/div , Y- axis 1 unit/div.) . . . . .	43
4.6	Rotor speed profile for Induction motor when a load of ( Scale: X-axis 5msec/div , Y-axis 500units/div.) . . . . .	44
4.7	Strategy to implement V/F method . . . . .	45
4.8	V/f generated signal shown in Oscilloscope ( Scale: X-axis 2sec/div , Y-axis 5v/div.) . . . . .	46
4.9	Induction motor rating. . . . .	46
4.10	Current profile when V/f supply is applied at 50Nm load.(Scale:Y-axis current in A,X-axis number of samples) . . . . .	46
4.11	Rotor speed with v/f supply at 50Nm load.(Scale: X-axis number of samples,Y-axis speed in rpm) . . . . .	47
4.12	Base values used for per unitization . . . . .	47
4.13	controller constants . . . . .	49
4.14	FLux angle estimation . . . . .	50



## ABBREVIATIONS

<b>FOC</b>	Field oriented control
<b>DC</b>	Direct current
<b>AC</b>	Alternating current
<b>PI</b>	Proportional and Integral
<b>VVF</b>	Variable voltage and frequency
<b>PWM</b>	Pulse width modulation
<b>VSI</b>	Voltage source Inverter
<b>RISC</b>	Reduced instruction set computing
<b>DSP</b>	Digital signal processor
<b>ePWM</b>	Enhanced pulse width modulation
<b>DAC</b>	Digital to analog converter
<b>ADC</b>	Analog to digital converter
<b>eCAP</b>	Enhanced capture
<b>TBPRD</b>	Time base period register
<b>TBCTR</b>	Time based counter
<b>CMP</b>	Compare
<b>MUX</b>	Multiplexer

## NOTATION

$\alpha$	Angle in degrees
$\beta$	Angle in degrees
$\omega$	Speed of motor
$\theta$	Angle in degrees
$\epsilon$	Electrical angle between stator and rotor axes
$\rho$	Angle of rotor flux axis wrt stator axis , $m$
$V_a$	Instantaneous a phase voltage
$V_b$	Instantaneous b phase voltage
$V_c$	Instantaneous c phase voltage
$I_a$	Instantaneous a phase current
$I_b$	Instantaneous b phase current
$I_c$	Instantaneous c phase current
$K_p$	Proportional constant in PI controller
$K_i$	Integrator constant in PI controller
$W_r$	rotor speed in electrical rad/sec
$W_{mr}$	synchronous speed in mechanical rad/sec
$R_s$	stator resistance
$R_r$	Rotor resistance
$L_s$	stator inductance
$L_r$	Rotor inductance
$L_{lr}$	Rotor leakage inductance
$L_{ls}$	stator leakage inductance
$L_m$	mutual inductance
$T_r$	Time constant for motor
$P$	No. of poles

# CHAPTER 1

## Separately excited DC motor speed control

### 1.1 Introduction

Direct current (DC) motors have been widely used in many industrial applications such as electric vehicles, steel rolling mills, electric cranes, and robotic manipulators due to precise, wide, simple, and continuous control characteristics . Here in this work we have implemented armature voltage control method for speed control which can be used to control the speed of motor below rated value(i.e) the drive is operated in constant Torque region . The desired Torque-speed characteristics of Motor is achieved by used of typical PI controller which is tuned according to the motor parameters. Simulation demonstrate the successful application of controller with dynamic changes.

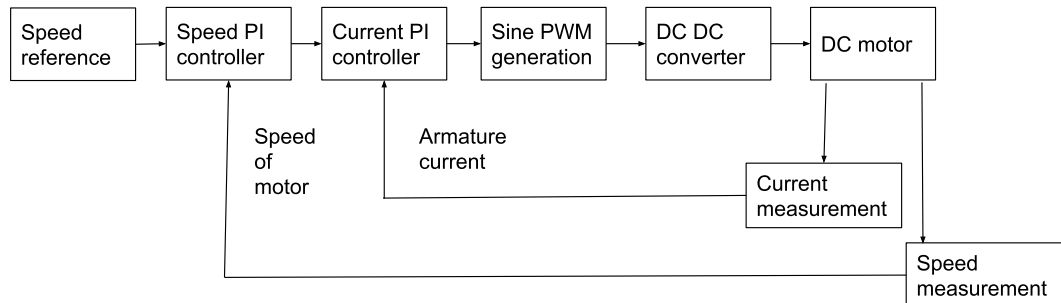


Figure 1.1: Block diagram for speed control of separately excited DC motor

From Block diagram shown in figure 1.1 we can see various building blocks required to implement control strategy, Where in Speed reference is the require speed input value. Based on the reference value input PI controllers act to stabilize the system. Hence proper controller constants calculation is key for functioning of control system.

## 1.2 Voltage speed control method

In Voltage speed control of a separately excited DC motor, The field current is kept constant (and hence the flux density  $B$  is constant), and the armature voltage is varied. A constant field current is obtained by separately exciting the field from a fixed dc source. The flux is produced by the field current, therefore essentially Flux is constant. Thus the torque is proportional only to the armature current. Here in this work we are using Voltage speed control. Hence, speed control below rated speed is Feasible.

Below given figure 1.2 shows the Torque vs Speed characteristic for DC motor. Stating we are operating in Constant torque and variable Power region until the rated value of speed is reached, As Speed goes above rated value voltage will cross the rated value as well. Therefore Owing to the Insulation breakdown voltage constraints we stick to this method upto when the speed of less than or equal to rated value is required.

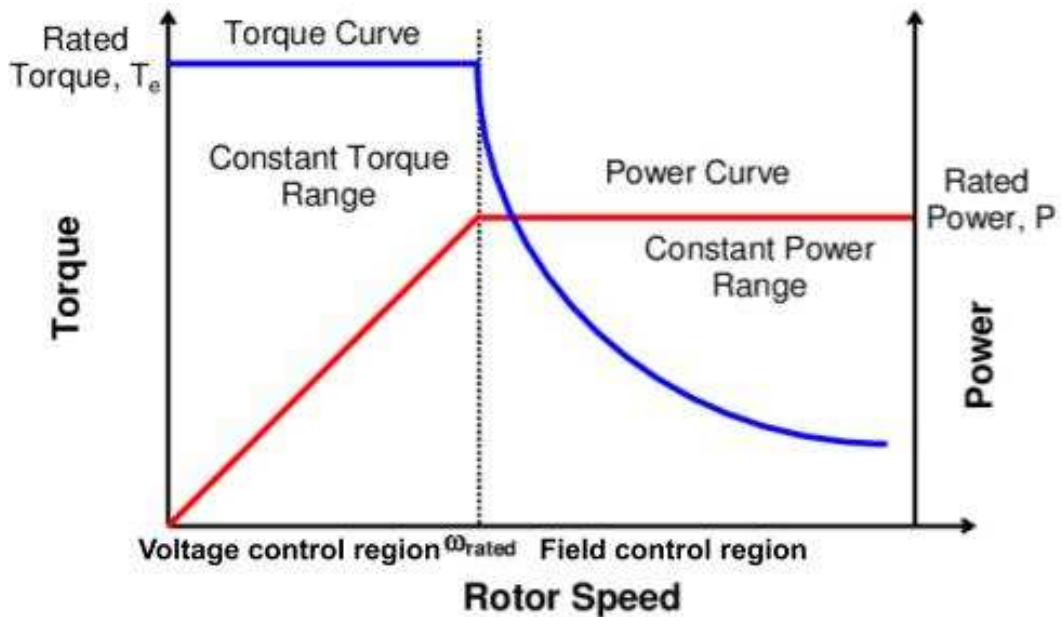


Figure 1.2: Torque vs Rotor speed plot for control strategies of separately excited DC motor.

### 1.3 Design of steady state model

Since we are going to control speed of separately excited DC motor with respect to the input armature voltage of the motor ,it is essential to get the related transfer function that is  $\frac{W(s)}{V_a(s)}$

Equations defining dynamics of separately excited DC motor

$$v_f = I_f R_f + L_f \frac{dI_f}{dt} \quad (1.1)$$

$$V_a = I_a R_a + L_a \frac{dI_a}{dt} + E_b \quad (1.2)$$

$$T_g - T_l = J \frac{dW}{dt} + BW \quad (1.3)$$

$$E_b = K I_f W \quad (1.4)$$

$$T_g = K I_f I_a \quad (1.5)$$

converting equation into state variable form with the given constraint of field being constant we have

$$\frac{dI_f}{dt} = 0 \quad (1.6)$$

$$\dot{X} = AX + BU \rightarrow (\text{State variable form})$$

Here we have  $i_a$  and  $W$  as state variable ,

$V_f, V_a, -T_l$  as input variables.

$$\begin{bmatrix} \frac{dI_a}{dt} \\ \frac{dW}{dt} \end{bmatrix} = \begin{bmatrix} \frac{-R_a}{L_a} & \frac{-K_f}{L_a} \\ \frac{K_f}{J} & \frac{-B}{J} \end{bmatrix} \begin{bmatrix} i_a \\ W \end{bmatrix} + \begin{bmatrix} \frac{1}{L_a} & 0 \\ 0 & -1 \end{bmatrix} \begin{bmatrix} V_a \\ T_l \end{bmatrix} \quad (1.7)$$

from (1.1)(1.2),(1.3),(1.4),(1.5)&(1.6)

also,we know that  $Y(s) = CX(s)$

here in our work  $Y(s)=W(s)$ ;

therefore

$$W(s) = \begin{bmatrix} 0 & 1 \end{bmatrix} \begin{bmatrix} i_a \\ W \end{bmatrix} \quad (1.8)$$

Transfer function is given by  $\frac{Y(s)}{U(s)} = C(SI - A)^{-1}B$

we obtain

$$\frac{W(s)}{Va(s)} = \frac{K_f}{(R_a + L_a S)(JS + B) + K_f^2} \quad (1.9)$$

but the above transfer function is without inverter gain ,considering inverter gain we have

$$G_c = \frac{K_c}{(1+ST_d)} \rightarrow \text{converter gain}$$

finally multiply equation (1.9) by  $G_c$

$$\frac{W(s)}{Va(s)} = \frac{K_f K_c}{(1 + ST_d)[(R_a + L_a S)(JS + B) + K_f^2]} \quad (1.10)$$

for lossy motor

considering ideal condition of lossless motor we get  $B=0, R_a=0$

$$\frac{W(s)}{Va(s)} = \frac{K_f K_c}{(1 + ST_d)[(L_a S)(JS) + K_f^2]} \quad (1.11)$$

we can see the from (1.10) and (1.11) transfer function becomes marginally stable when considered lossless as compared to stable system with losses hence losses are essential part of the system for controller.

## 1.4 Design of Controllers

### 1.4.1 Current Controller

Depending on the switching frequency of the converter we choose the bandwidth of the current controller loop

Lets say we have  $f_s$  as switching frequency. We choose bandwidth of the controller as  $f_s/10$  for good response.

given is the current controller loop shown in figure(1.3)

We design the loop transfer function to have first order .so as to get faster response with zero oscillations.

therefore

open loop transfer function

$$\frac{i_a}{i_a^*} = \frac{1}{sT_b} = \frac{K_{pi}(1 + sT_i)G_i}{R_s(1 + sT_s)(sT_{pi})} \quad (1.12)$$

where  $G_i$  is inverter constant,  $T_b$  is the current controller bandwidth.

$$T_s = \frac{L_a}{R_a}$$

$T_s$  is rotor time constant.

for the loop transfer function to be first order we choose  $T_{pi} = T_s$ .

$$\text{hence } K_{pi} = \frac{L_a}{V_{ds}T_b} \rightarrow T_b = \frac{1}{2\pi f_b}$$

$$K_i = \frac{K_p}{T_{pi}}$$

$k_p$  is proportional controller gain.  $k_i$  is integral controller gain.

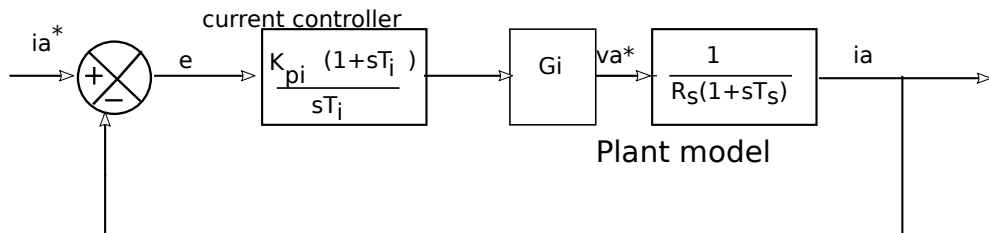


Figure 1.3: Current controller loop for separately excited DC motor.

Figure 1.3 shows inner controller loop for the speed control of Dc motor. Current controller gets the reference input from the outer controller loop which is the speed loop, this reference value is processed through PI controller to generate reference signal for generation of Converter pulses ,Here we have used Sine PWM method. Finally converter output is given to DC motor which is represented by transfer function as plant model.

### 1.4.2 Speed controller

Speed control loop is the outer loop of current controller whose bandwidth should be very small as compared to the current loop as can be given by  $f_s/100$ .

the figure (1.4) shows the speed control loop.

since current loop is designed as first order system we use equivalent first order system for current loop.

loop transfer function for speed loop

$$G_c(s) = \frac{K_{pw}(1+ST_{Wpi})K_f}{S^2JT_{Wpi}(1+ST_{pi})}$$

for such a system we define the controller parameters using method of symmetric optimum pole placement so as to obtain maximum phase angle at gain crossover frequency.

figure(1.5) shows the bode plot for the transfer function given above. Thus we design controller such that the system gain crosses the 0dB point at this frequency with a slope of -20dB/decade. Thus once we choose  $f_{bw}$  appropriately ,the value of  $f_w$  can be calculated as  $f_{bw}^2 = f_w f_{bi}$

we get

$$K_{pw} = \frac{2\pi f_{bw} J}{k_{pw} K_f}$$

$$K_{iw} = \frac{K_p}{T_w}$$

Figure 1.4 shows the Speed controller loop for DC motor speed control. Speed reference  $\omega^*$  is the required speed to be obtained from motor output.  $M_l$  is the load torque to be given as input for the system based on loading given.



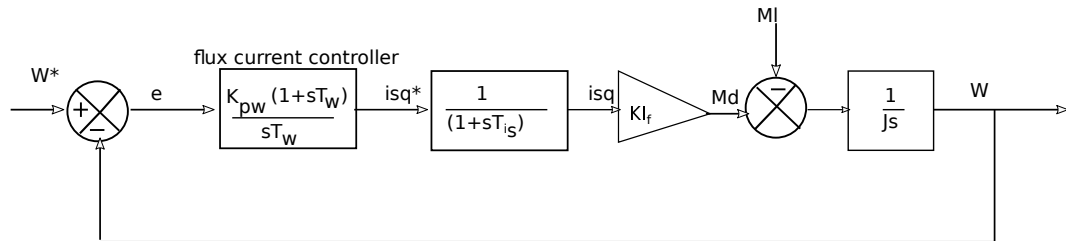


Figure 1.4: Speed controller loop for separately excited DC motor

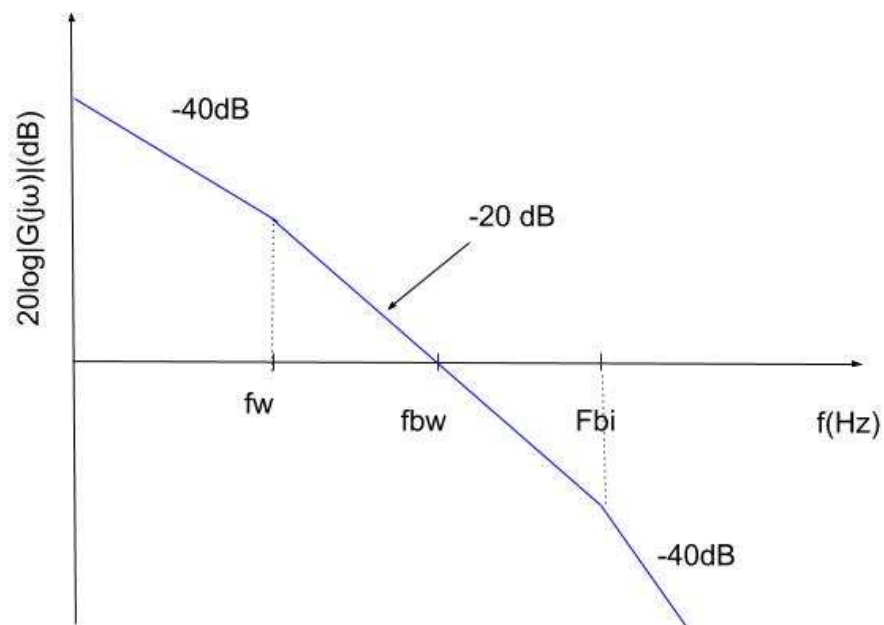


Figure 1.5: Bode plot depicting symmetric optimum pole placement.

figure 1.5 represents Bode plot to be developed to implement proper control strategy. Since we will initially decide inner control loop bandwidth  $F_{bi}$  and  $F_{bw}$  as given in subsection 1.4, According to symmetric optimum pole placement method we place the bandwidth of the system,  $F_w$  should be designed such that the bode plot crosses 0dB gain at  $F_{bw}$ .

## 1.5 Simulation results

Simulation was carried out in MATLAB Simulink for the given motor with parameters and calculated controller constants shown in figure (1.6)

Parameter	label	Value
Ra	Armature resistance	1.13Ω
La	Armature Inductance	12.16mH
Kpw	Speed proportional constant	6.2
Kiw	Speed Integral constant	0.03084
Kpi	Current proportional constant	0.127
Kii	Current integral constant	11.80
Kt	Motor torque constant	1.076Nm/A
Ke	Motor EMF constant	1.076Nm/A
B	Motor viscosity	0.0034Nm
J	Moment of Inertia	0.0425Kgm <sup>2</sup>
Tl	Rated load torque	40.77Nm
Vm	Rated voltage	240V
Pm	Rated Power	10HP
Wm	Rated speed	1750rpm

Figure 1.6: DC motor parameters.

and simulation results for current (fig. 1.7) and speed (fig. 1.8) are given. (for step change in load at  $t=1\text{sec}$ )

Figure 1.7 represents current profile for DC motor with step change in load at  $t=1\text{sec}$ . Here Step change in load implies initially motor was started at no load and at  $t=1\text{sec}$  full load for motor is applied, from figure it can be seen that at no load Current is zero and as soon as the load is applied the current profile seems to be settling instantly at the rated value of armature current.

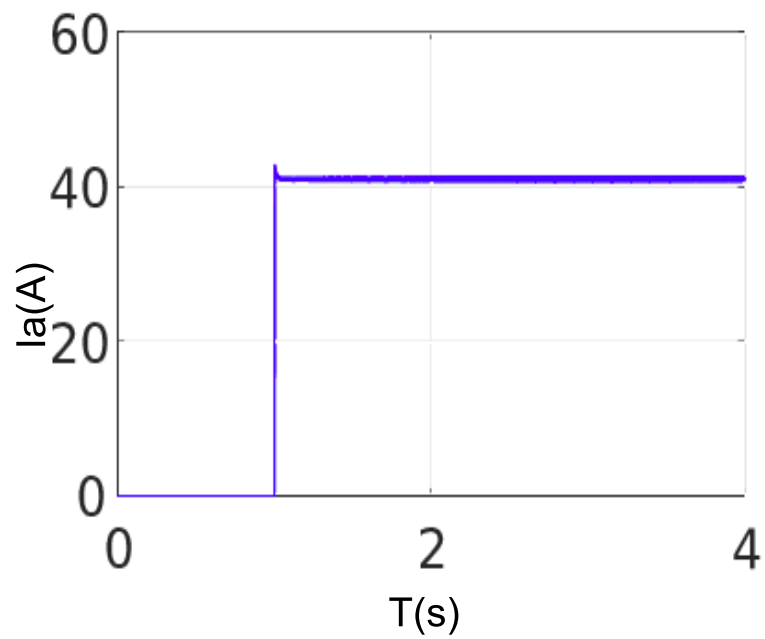


Figure 1.7: DC motor speed plot when full load torque is applied at  $t=1$  sec. (Scale: X-axis 2sec/div ,Y-axis 20A/div)

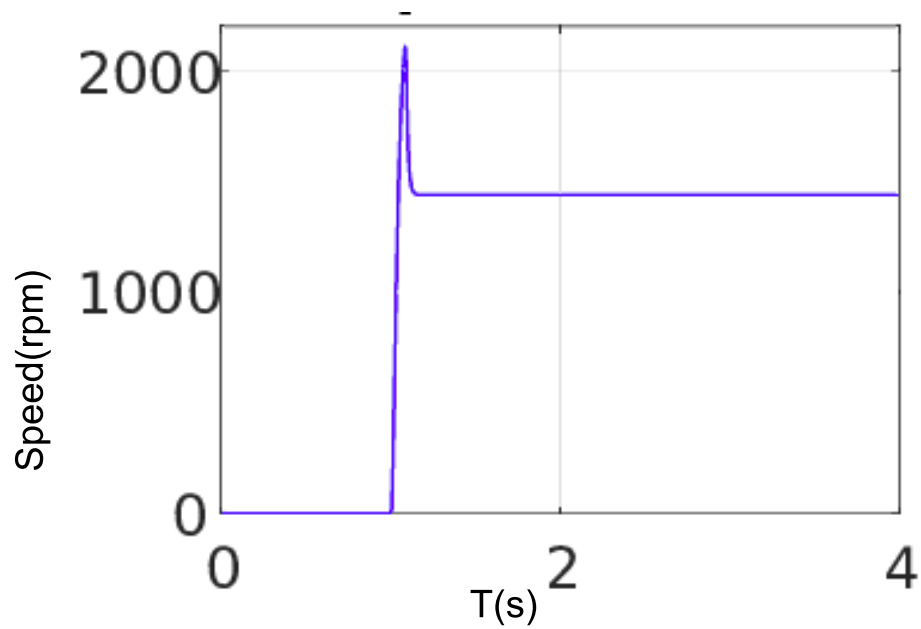


Figure 1.8: DC motor speed profile when supply is given at  $t=1$ sec at full load torque, with speed reference of 1400rpm. ( Scale: X-axis 2sec/div ,Y-axis -1000rpm/div.)

figure 1.8 shows speed profile when Supply is given to motor at  $t=1\text{sec}$  at full load torque ,It can be seen from the profile that the Speed rises almost instantly to the given reference value of 1400rpm. Overshoot in the speed profile can be due to timing mismatches of controllers or calculation approximations.

# CHAPTER 2

## Vector control of Induction motor

### 2.1 Introduction

Since the emergence of Induction motor it has dominated the Industrial market owing to the fact that it is Self-starting, reliable economic, robust and has simple structure. However for Industrial purpose we need Variable speed operation which lead to VVF method. where in (V/f) ratio is maintained constant to maintain flux inside the motor to be below rated value. But the fact that this method gave very poor dynamic response . which paved way for development of superior technique and based on the fact that separately excited motors can be controlled by two components armature voltage and field voltage. Vector Control was developed which emulates Separately excited DC motor speed control.

### 2.2 Vector Control

Vector control is a variable-frequency drive (VFD) control method in which the stator currents of a three-phase AC Induction motor are transformed into two orthogonal components which can be seen as a 2 vectors. One component defines the magnetic flux of the motor, the other the torque. The control system of the drive calculates the corresponding current component references from the flux and torque references given by the drive's speed control. Typically proportional-integral (PI) controllers are used to keep the measured current components at their reference values. The pulse-width modulation of the variable-frequency drive defines the transistor switching according to the stator voltage references that are the output of the PI current controllers.

Vector control is used to control AC synchronous and induction motors. It was originally developed for high-performance motor applications that are required to operate smoothly over the full speed range, generate full torque at zero speed, and have high



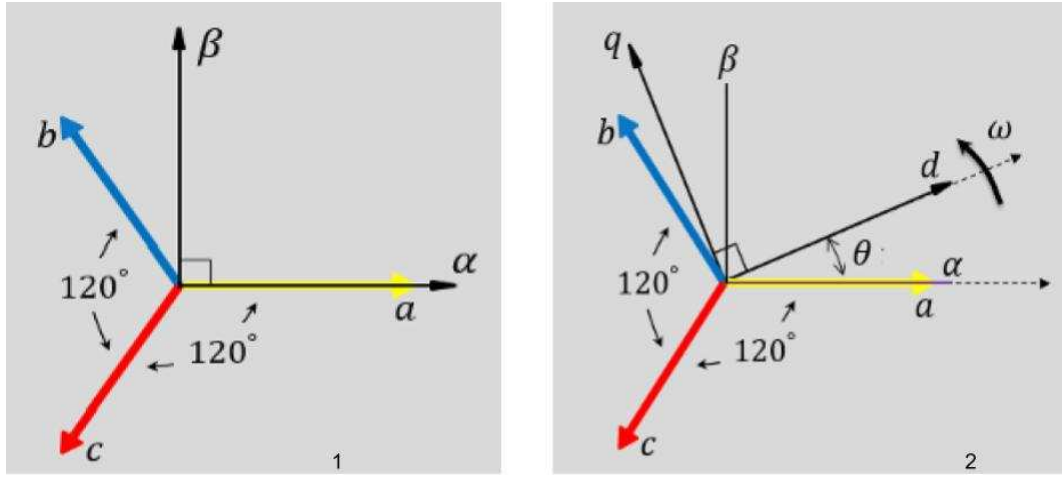


Figure 2.2: In figure 2.2, Figure 1 represents Clarke's transform and Figure 2 represents Park's transform

### 2.2.2 Park's transformation

Park Transform converts the time-domain components of a three-phase system in an  $\alpha, \beta$  reference frame to direct, quadrature, and zero components in a rotating reference frame. The transform can preserve the active and reactive powers with the powers of the system in the abc reference frame by implementing an invariant version of the Park transform. For a balanced system, the zero component is equal to zero.

You can configure the transform to align at any angle  $\theta$  with  $\alpha$  or  $\beta$ -axis of the system to either the d- or q-axis of the rotating reference frame at time,  $t = 0$ . Below given is the mathematical conversion of ab to d-q transformation.

$$\begin{bmatrix} I_\alpha \\ I_\beta \end{bmatrix} = \begin{bmatrix} \cos(\theta) & \sin(\theta) \\ -\sin(\theta) & \cos(\theta) \end{bmatrix} \begin{bmatrix} I_d \\ I_q \end{bmatrix}$$

Park transform represents rotating frame of reference since the angle  $\theta$  keeps on changing with respect to time for a given 3 phase balanced quantities.

In our work we have chosen Rotor flux reference frame therefore the angle  $\rho_{mr}$  will be the changing with respect to  $\alpha$  or  $\beta$  ( $\alpha, \beta$  being stationary) as rotor flux rotates with some angular speed  $\omega_{mr}$ .

Figure 2.3 represents required phasor for implementation of Vector control. Intentionally we choose d-axis as the rotor flux axis which can be seen to rotate at the given synchronous speed of motor  $\omega_{mr}$ . And the rotor flux axis can be seen to have a phase difference of  $\rho_{mr}$  since Rotor flux axis rotates our phase angle  $\rho_{mr}$  keeps on

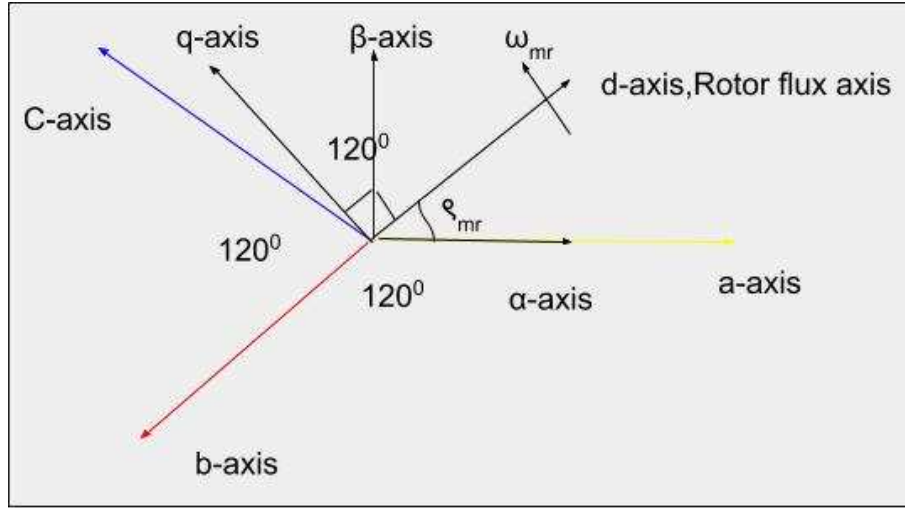


Figure 2.3: Phasor diagram for Vector control.

changing.hence continuous tracking of rotor flux angle is key to Vector control implementation.

### 2.2.3 Power Inverter(VSI)

An inverter is an Power electronics circuitry which converts DC voltage to AC voltage. PWM scheme is used for switching of Power devices used in it.Power Electronic Inverters are used where high rating of voltage and currents are to be handled.The inverter does not produce any power by itself ,its power is generated from the input side DC source.where as the input voltage,output voltage ,frequency of operation can vary from topology to topology being used in the operation.

Here in this work the required input to the Induction motor is 380V(L-L)Rms i.e the Inverter has to produce fundamental of 380V at the output .

Since we have used Sine PWM technique for switching of devices we get the minimum input voltage required for maximum phase voltage of

$$V_{ph} = 380 * \sqrt{\frac{2}{3}} = 310.26v$$

Therefore,according to SPWM method

$$V_{ph} = m_a * \frac{V_{dc}}{2}$$

$$\Rightarrow V_{dc} = 2 * V_{ph} * m_a$$



considering  $m_a \rightarrow \text{Modulation index}(0.8)$

$$V_{dc} = 2 * 310.26 * \frac{1}{0.8} = 775\text{V}$$

Safety margin constraints we take  $V_{dc} = 800\text{V}$

## 2.2.4 Mathematical modeling

### Space Phasor modeling of Induction motor in Rotor Flux reference Frame:

Space phasor can be defined as the equivalent of certain set of phasor quantities in space. Let's say we have set to 3 phase currents  $I_a, I_b, I_c$  which are equal in magnitude and 120 degree apart (abc phase sequence).

Space phasor for such quantities is given as

$$i_s^-(t) = i_{sa}(t) + i_{sb}(t)e^{j(2\pi/3)} + i_{sc}(t)e^{-j(2\pi/3)} \quad (2.1)$$

Similar concept has been used in this work for to formulate flux, stator voltage, and stator current equations of SCIM.

The stator and rotor voltage equations can be written as

$$V_s^-(t) = R_s i_s(t) + \frac{d\psi_s^-(t)}{dt} \quad (2.2)$$

$$V_r^-(t) = R_r i_r(t) + \frac{d\psi_r^-(t)}{dt} \quad (2.3)$$

These above given 2 equations represent electrical behaviour of the machine where

$\psi_s(t) \rightarrow$  flux generating component in stator domain.

$\psi_r(t) \rightarrow$  flux generating component in rotor domain.

where

$$\bar{\psi}_s(t) = L_s \bar{i}_s(t) + L_m (i_r(t) e^{j\epsilon(t)}) \quad (2.4)$$

$$\bar{\psi}_r(t) = L_r \bar{i}_r(t) + L_m(\bar{i}_s(t)e^{-j\epsilon(t)}) \quad (2.5)$$

$\epsilon \rightarrow$ Electrical angle between stator and rotor axes.

therefore voltage equations can be modified as

$$\bar{V}_s(t) = R_s \bar{i}_s(t) + L_s \frac{d\bar{i}_s(t)}{dt} + L_m \frac{d\bar{i}_r(t)e^{j\epsilon(t)}}{dt} \quad (2.6)$$

$$0 = R_r \bar{i}_r(t) + L_s \frac{d\bar{i}_r(t)}{dt} + L_m \frac{d\bar{i}_s(t)e^{-j\epsilon(t)}}{dt} \quad (2.7)$$

These 2 equation given above represent space phasor equivalent circuit of squirrel cage Induction motor. In squirrel cage IM rotor bars are short circuited through end rings hence  $V_r = 0$ , given circuit shows the space phasor model of motor referred to stator domain.

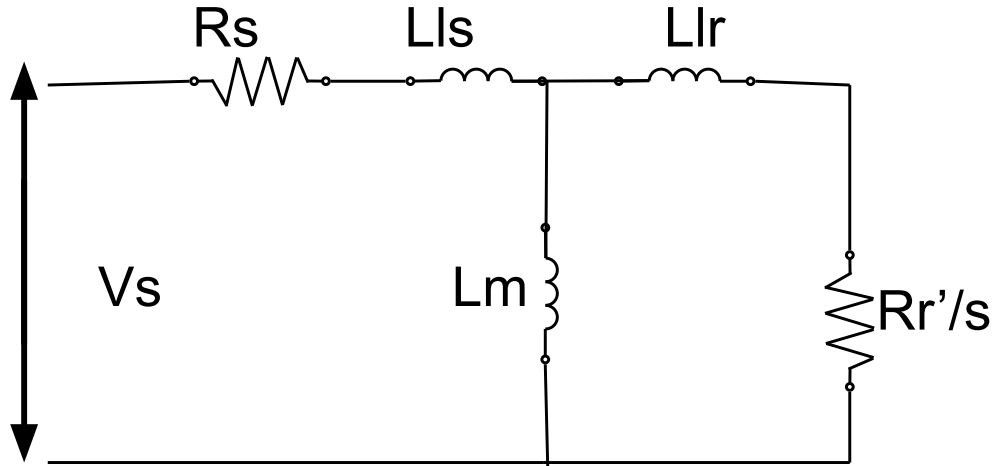


Figure 2.4: Equivalent circuit of Induction motor in Space Phasor domain.

### **Torque expression:**

Torque expression in terms of Space phasor quantities referred to stator windings can be derived as

voltage equations referred to stator windings are

$$\begin{bmatrix} V_{abc}^s \\ 0 \end{bmatrix} = \begin{bmatrix} R_s + \sigma L_s & \sigma L_{rs} \\ (Lr_s)^T & L_r \end{bmatrix} \begin{bmatrix} i_{abc}^s \\ i_{abc}^r \end{bmatrix} \quad (2.8)$$

where  $\begin{bmatrix} V_{abc}^s \end{bmatrix} = \begin{bmatrix} V_{sa} & V_{sb} & V_{sc} \end{bmatrix}^T$  represent stator phase voltage vector.

where  $\begin{bmatrix} i_{abc}^s \end{bmatrix} = \begin{bmatrix} i_{sa} & i_{sb} & i_{sc} \end{bmatrix}^T$  represent stator current vector.

where  $\begin{bmatrix} i_{abc}^r \end{bmatrix} = \begin{bmatrix} i_{ra} & i_{rb} & i_{rc} \end{bmatrix}^T$  represent rotor current vector.

$R_r, R_s$  represent stator and rotor resistance diagonal matrices.

$$L_s = \begin{bmatrix} L_{ls} + L_{ms} & -0.5L_{ms} & -0.5L_{ms} \\ -0.5L_{ms} & L_{ls} + L_{ms} & -0.5L_{ms} \\ -0.5L_{ms} & -0.5L_{ms} & L_{ls} + L_{ms} \end{bmatrix} \quad (2.9)$$

$$Lr = \begin{bmatrix} L_{lr} + L_{ms} & -0.5L_{ms} & -0.5L_{ms} \\ -0.5L_{ms} & L_{ls} + L_{ms} & -0.5L_{ms} \\ -0.5L_{ms} & -0.5L_{ms} & L_{lr} + L_{ms} \end{bmatrix}, \quad (2.10)$$

$$Lsr = \begin{bmatrix} \cos\epsilon & \cos(\epsilon + 2\pi/3) & \cos(\epsilon - 2\pi/3) \\ \cos(\epsilon - 2\pi/3) & \cos\epsilon & \cos(\epsilon + 2\pi/3) \\ \cos(\epsilon + 2\pi/3) & \cos(\epsilon - 2\pi/3) & \cos\epsilon \end{bmatrix} \quad (2.11)$$

where

$L_{ls}$  is Stator leakage Inductance.

$L_{lr}$  is Rotor leakage Inductance.

$L_{ms}$  is Stator magnetizing Inductance.

Now,

Stored energy in the coupling filed , $W_f$  can now be written as

$$W_f = 0.5 \begin{bmatrix} i_{abc}^s \end{bmatrix}^T \begin{bmatrix} L_s - L_{ls} I \end{bmatrix} \begin{bmatrix} i_{abc}^s \end{bmatrix} + \begin{bmatrix} i_{abc}^s \end{bmatrix} \begin{bmatrix} L_{rs} \end{bmatrix} \begin{bmatrix} i_{abc}^r \end{bmatrix} + 0.5 \begin{bmatrix} i_{abc}^r \end{bmatrix} \begin{bmatrix} L_r - L_{lr} I \end{bmatrix} \begin{bmatrix} i_{abc}^r \end{bmatrix} \quad (2.12)$$

where I denotes identity matrix. Neglecting saturation effect and assuming a linear magnetic system, field energy is equal to the co-energy,  $W_c$ . The torque is obtained as the partial derivative of the co-energy with the mechanical angle.

thus Torque can be given as

$$M_d = \frac{dW_c(i, \epsilon)}{d\theta_m}$$

where  $\theta_m = \frac{2}{P} \epsilon$

therefore evaluating  $M_d$  gives

$$M_d = -\frac{1}{2} \frac{P}{2} L_{ms} \begin{bmatrix} i_{abc}^s \end{bmatrix}^T \begin{bmatrix} \sin \epsilon & \sin(\epsilon + 2P/3) & \sin(\epsilon + 2P/3) \\ \sin(\epsilon + 2P/3) & \sin \epsilon & \sin(\epsilon + 2P/3) \\ \sin(\epsilon + 2P/3) & \sin(\epsilon + 2P/3) & \sin \epsilon \end{bmatrix} \begin{bmatrix} i_{ra} \\ i_{rb} \\ i_{rc} \end{bmatrix} \quad (2.13)$$

$$\text{put } \sin \epsilon = \frac{e^{j\epsilon} - e^{-j\epsilon}}{2j}$$

we get,

$$M_d = \frac{-1}{2j} \frac{P}{2} L_{ms} \left[ \bar{i}_r \bar{i}_s^* e^{j\epsilon} - \bar{i}_s \bar{i}_r^* e^{-j\epsilon} \right]$$

where  $\bar{i}_r, \bar{i}_s$  — — > are rotor current and stator current space Phasors

simplifying  $M_d$  equation gives

$$M_d = \frac{1}{2j} \frac{P}{2} L_{ms} \left[ \bar{i}_s \bar{i}_r^* e^{-j\epsilon} - \bar{i}_r \bar{i}_s^* e^{j\epsilon} \right] = \frac{P}{2} L_{ms} \{ \text{Im}g[\bar{i}_s (\bar{i}_r e^{j\epsilon})^*] \} \quad (2.14)$$

substituting  $L_m = \frac{3}{2} L_{ms}$

we get,

$$Md = \frac{2}{3} \frac{P}{2} L_m \{ \text{Im}g[\bar{i}_s(\bar{i}_r e^{j\epsilon})^*] \} \quad (2.15)$$

This is the final expression for machine torque where all the quantities are in their respective coordinates.

$$\bar{V}_s(t) = R_s \bar{i}_s(t) + L_s \frac{d\bar{i}_s(t)}{dt} + L_m \frac{d\bar{i}_r(t) e^{j\epsilon(t)}}{dt} \quad (2.16)$$

$$0 = R_r \bar{i}_r(t) + L_s \frac{d\bar{i}_r(t)}{dt} + L_m \frac{d\bar{i}_s(t) e^{-j\epsilon(t)}}{dt} \quad (2.17)$$

$$J \frac{d\omega_m}{dt} + B\omega_m = \frac{2}{3} \frac{P}{2} L_m \{ \text{Im}g[\bar{i}_s(\bar{i}_r e^{j\epsilon})^*] \} - Ml. \quad (2.18)$$

Equations(28),(29),(30) give above defines the behaviour of machine under transient as well as steady state.

### Equations defining control:

Since in the introduction part we have learned that to achieve decoupled speed and torque control ,the current components  $i_{sd}$  and  $i_{sq}$  needs to be controlled and the basic drive structure is shown earlier in the Introduction part. We will derive certain important equation here:

Rotor voltage equation

$$0 = R_r \bar{i}_r(t) + L_s \frac{d\bar{i}_r(t)}{dt} + L_m \frac{d(\bar{i}_s(t) e^{-j\epsilon(t)})}{dt}$$

which can be written as,

$$0 = R_r \bar{i}_r(t) + (1 + \sigma_r) L_m \frac{d\bar{i}_r(t)}{dt} + L_m \frac{d(\bar{i}_s(t) e^{-j\epsilon(t)})}{dt}$$

where

$$\sigma_r = \frac{L_{lr}}{L_m} \implies (1 + \sigma_r)L_m = L_r \quad (2.19)$$

Rotor flux phasor in rotor coordinates is given by

$$\bar{\psi}_r(t) = (1 + \sigma_r)L_m i_r(t) + L_m(\bar{i}_s(t)e^{-j\epsilon(t)})$$

therefor rotor flux phasor in stator coordinates can be obtained by multiplying with  $e^{j\epsilon(t)}$

$$\bar{\psi}_r(t)e^{j\epsilon(t)} = L_m((1 + \sigma_r)\bar{i}_r(t)e^{j\epsilon(t)} + (\bar{i}_s(t))) = L_m\bar{I}_{mr}(t)$$

where ,

$$\bar{I}_{mr}(t) = \bar{i}_s(t) + (1 + \sigma_r)\bar{i}_r(t)e^{j\epsilon(t)}$$

therefore  $\bar{i}_r(t)$  can be written as

$$\bar{i}_r(t) = \frac{(\bar{i}_{mr}(t) - \bar{i}_s(t))}{(1 + \sigma_r)}e^{-j\epsilon(t)}$$

Substituting this in Rotor voltage equation

$$0 = R_r \frac{(\bar{i}_{mr}(t) - \bar{i}_s(t))}{(1 + \sigma_r)}e^{-j\epsilon(t)} + L_m \frac{d}{dt} \left[ \frac{(\bar{i}_{mr}(t) - \bar{i}_s(t))}{1} e^{-j\epsilon(t)} \right] + L_m \frac{d(\bar{i}_s(t)e^{-j\epsilon(t)})}{dt}$$

$$0 = R_r \frac{(\bar{i}_{mr}(t) - \bar{i}_s(t))}{(1 + \sigma_r)}e^{-j\epsilon(t)} + \left[ L_m \frac{d\bar{i}_{mr}(t)}{dt} - j \frac{d\epsilon(t)}{dt} \bar{i}_{mr}(t) L_m \right] e^{-j\epsilon(t)}$$

above equations is in rotor coordinates multiplying by  $e^{j\epsilon(t)}$  to transform into stator coordinates and  $\frac{d\epsilon(t)}{dt}$  gives speed of rotor in electrical rad/sec.

$$\Rightarrow 0 = R_r \frac{(\bar{i}_{mr}(t) - \bar{i}_s(t))}{(1 + \sigma_r)} + \left[ L_m \frac{d\bar{i}_{mr}(t)}{dt} - j \omega \bar{i}_{mr}(t) L_m \right]$$

since this equation is in stator frame we transform it into rotor flux frame.

$$i_{mr}^-(t) = i_{mr}(t)e^{j\rho(t)} \quad (2.20)$$

where

$\rho(t) \rightarrow$ denotes instantaneous rotor position of rotor flux space vector w.r.t the stator axis.

therefore substituting  $i_{mr}$  and multiplying by  $e^{-j\rho(t)}$  evaluating equation implies

$$R_r \frac{(i_s(t))}{(1+\sigma_r)} = R_r \frac{(i_{mr}^-(t))}{(1+\sigma_r)} e^{j\rho(t)} + [L_m \frac{di_{mr}^-(t)}{dt} - j(\omega_{mr}-\omega)i_{mr}(t)L_m]$$

where  $\omega_{mr} = \frac{d\rho(t)}{dt}$  in stator coordinates and can be transformed into rotor flux coordinates by multiplying  $e^{-j\rho(t)}$ .

Thus we get

$$R_r \frac{(i_s(t))}{(1+\sigma_r)} e^{-j\rho(t)} = R_r \frac{(i_{mr}^-(t))}{(1+\sigma_r)} e^{j\rho(t)} + [L_m \frac{di_{mr}^-(t)}{dt} - j(\omega_{mr}-\omega)i_{mr}(t)L_m]$$

above equation is for stator current in rotor flux coordinates.

let  $i_{sd}$  and  $i_{sq}$  denotes component of stator current phasor in rotor flux coordinates.

therefore

$$R_r \frac{(i_{sd}(t) + j i_{sq}(t))}{(1+\sigma_r)} = R_r \frac{(i_{mr}^-(t))}{(1+\sigma_r)} e^{j\rho(t)} + [L_m \frac{di_{mr}^-(t)}{dt} - j(\omega_{mr}-\omega)i_{mr}(t)L_m]$$

separating real and imaginary parts and simplifying we get

$$i_{sd}(t) = i_{mr}(t) + \tau_r \frac{di_{mr}(t)}{dt} \quad (2.21)$$

$$\omega_{slip} = \frac{i_{sq}(t)}{\tau_r i_{mr}(t)} \quad (2.22)$$

where  $\tau_r \rightarrow \frac{L_m(1+\sigma_r)}{R_r}$

also, substituting  $\bar{i}_r(t)$  in  $M_d$  equation

we have

$$M_d = \frac{2}{3} \frac{P}{2} \frac{L_m}{1 + \sigma_r} i_{mr}(t) i_{sq}(t) \quad (2.23)$$

equation (2.21), (2.22), (2.23) represents set of dynamic equations on IM in rotor flux frame.

from these equations we can infer that

1. In steady state  $i_{mr}$  and  $i_{sd}$  are same .
2. The torque equation can be seen to have similarities with the torque equation for DC machine.

### Stator dynamics in rotor flux frame:

Stator voltage equation can be given by

$$\bar{V}_s(t) = R_s \bar{i}_s(t) + L_s \frac{d\bar{i}_s(t)}{dt} + L_m \frac{d\bar{i}_r(t) e^{j\epsilon(t)}}{dt} \text{ in stator frame.}$$

substituting  $\bar{i}_r(t)$

$$\bar{V}_s(t) = R_s \bar{i}_s(t) + L_s \frac{d\bar{i}_s(t)}{dt} + \frac{L_m}{(1+\sigma_r)} \frac{d[\bar{i}_{mr}(t) - i_s(t)]}{dt}$$

transforming above equation to rotor coordinate by multiplying  $e^{-j\rho(t)}$

$$\bar{v}_s^r(t) = v_{sd}(t) + jv_{sq}(t)$$

$$\text{and } \bar{i}_s^r(t) = i_{sd}(t) + ji_{sq}(t)$$

therefore

$$v_{sd}(t) + jv_{sq}(t) = R_s(i_{sd}(t) + ji_{sq}(t)) + L_s\left[\left(\frac{di_{sd}(t)}{dt} + j\frac{di_{sq}(t)}{dt}\right) + ji_{sd}(t)\omega_{mr} - i_{sq}(t)\omega_{mr}\right] + \frac{L_m}{1+\sigma_r}\left[\frac{d}{dt}(i_{mr}(t) - i_{sd}(t)) - j\frac{di_{sq}(t)}{dt} + j\omega_{mr}(i_{mr} - i_{sd}) + i_{sq}\omega_{mr}\right]$$

separating real and imaginary part and simplifying them

$$v_{sd} = R_s i_{sd} + \sigma L_s \frac{di_{sd}}{dt} - \sigma L_s i_{sq} \omega_{mr} + (1 - \sigma) L_s \frac{di_{mr}}{dt}$$



$$v_{sq} = R_s i_{sq} + \sigma L_s \frac{di_{sq}}{dt} - \sigma L_s i_{sd} \omega_{mr} + (1 - \sigma) L_s i_{mr} \omega_{mr}$$

where  $\sigma = 1 - \frac{L_m^2}{L_s L_r}$  is leakage factor.

Hence the above obtained  $v_{sd}, v_{sq}$  equations can be used to calculate required values of the d and q axis stator volts which are then realised using a SPWM VSI.

feed forward terms to improve the response of the d and q axis currents of the respective voltages are given by

$$v_{ffd} = -\sigma L_s i_{sq} \omega_{mr} + (1 - \sigma) L_s \frac{di_{mr}}{dt} \quad (2.24)$$

$$v_{ffq} = \sigma L_s i_{sd} \omega_{mr} + (1 - \sigma) L_s \omega_{mr} i_{mr} \quad (2.25)$$

the addition of these terms to the output of the d-axis and q-axis current controller respectively gives a first order response of the dq axis currents to the respective dq axis voltages.

## 2.2.5 Design of Controllers:

We have used PI controllers in our system for d-axis current, q-axis current flux and speed control. Controllers are the important part of the system therefore it is essential to tune them properly.

we have neglected Inverter delay, the bandwidth of the outer loop are much smaller than the inner loop so as to get proper dynamics.

### PI controller:

The Pi controllers used in our system are provided with output limiters and integrator anti-windup. Output limiters ensure that the parameters to be controlled for the machine are within the limits. The integrator anti-windup disables the integral action when the

output of the controller reaches its desired value making it faster and reliable.

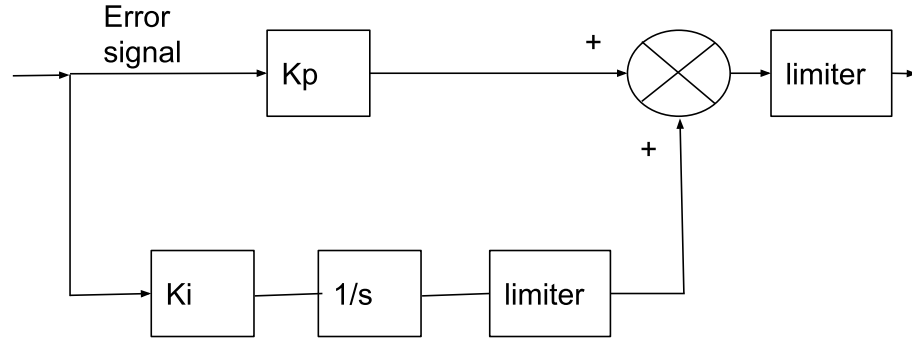


Figure 2.5: Anti-windup PI controller block diagram.

### d and q axis current controllers

we have designed controller such that the operation its loop time should be faster than the flux and speed controller. Both the current controllers will have same dynamics and constant since the inner loop deals with inverter and the machine.

consider bandwidth of thr loop to be  $f_b$ Hz.

$$\text{therefor } t_b = \frac{1}{2\pi f_b}$$

we choose the parameters of the controller such that the overall loop transfer function should be first order .

owing to tha fact that first order response is non oscillatory and fast.

$$\frac{K_p(1+sT_{id})}{sT_{id}} * G_i * \frac{1}{Rs(1+sT_s)} = \frac{1}{sT_b}$$

$$T_s = \frac{\sigma L_s}{R_s}, \text{ choose } T_{id} = T_s,$$

$$\text{gives } K_p = \frac{R_s T_s 2\pi f_b}{G_i}$$

$G_i \rightarrow$  Inverter gain

for Integral term

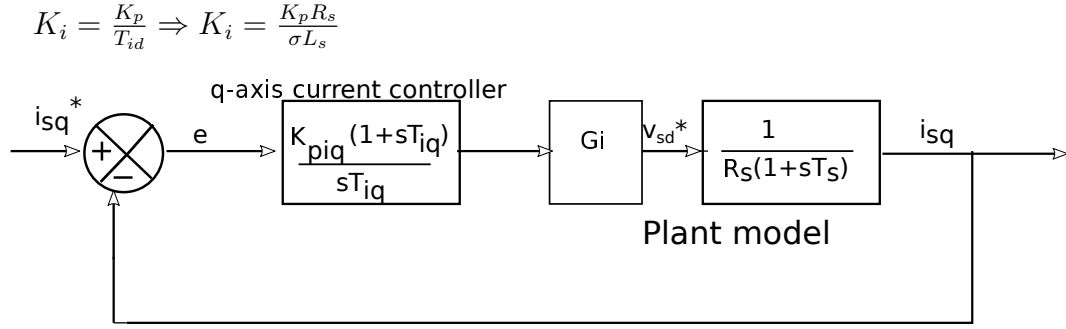


Figure 2.6: Figure represents q - axis current controller loop,d-axis current loop will be similar to this.

### Flux controller

It is controlled by controlling  $i_{mr}$ , which denotes magnetising component of current. Hence the output of flux controller will give d-axis current. Bandwidth for this loop will be chosen such that it is much lower than the current controller bandwidth. (choosing its bandwidth as 1/10th of current loop)

Let its bandwidth be  $f_{bmr}$  Hz,

$$T_{bmr} = \frac{1}{2\pi f_{bmr}}$$

loop transfer function should be first order hence formulating condition by

$$\frac{K_{pimr}(1+sT_{imr})}{sT_{imr}} * \frac{1}{(1+sT_r)} = \frac{1}{sT_{bmr}}$$

where  $T_r = \frac{L_r}{R_r}$  and choosing  $T_{imr} = T_r$

we have  $K_{pimr} = \frac{T_r}{T_{bmr}}$

$$K_{imr} = \frac{K_{pimr}}{T_r} = \frac{1}{T_{bmr}}$$

### Speed controller

Output of speed PI controller is the reference value for the q-axis current. Since the current loop is designed in the above sections its equivalent first order transfer function

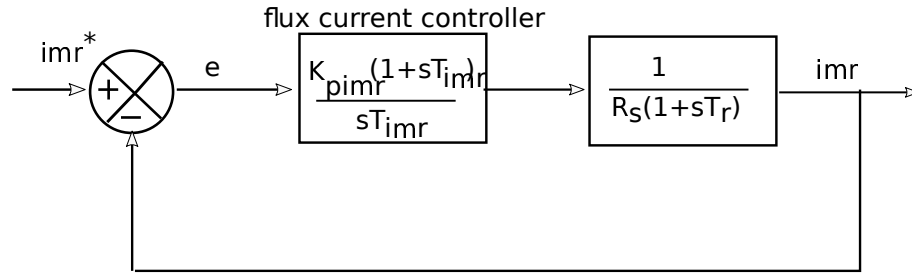


Figure 2.7: Flux controller loop.

is used in this part for design.(choosing its bandwidth as 1/10th of current loop)

The design of this loop is done using symmetric optimum pole placement method, the objective of this method is to obtain maximum phase angle at gain cross over frequency, from the block diagram the open loop transfer function can be given by

$$G(s) = \frac{K_p K_t i_{mr}^* (1 + s T_w)}{J T_w s^2 (1 + s T_w)}$$

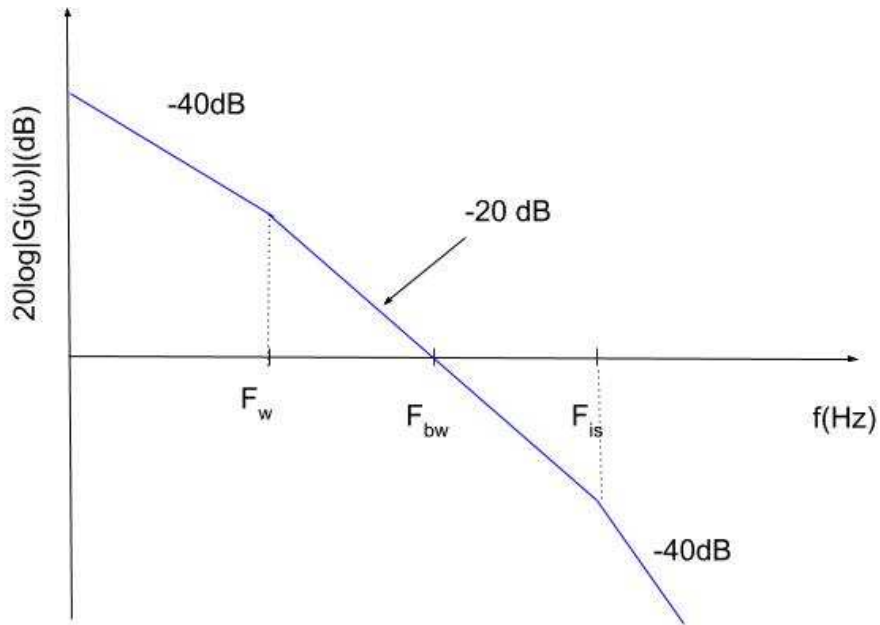


Figure 2.8: Bode plot for symmetric optimum pole placement.

the bode plot of this transfer function has the form shown in fig.11 for such a system maximum phase angle can be shown to occur at the geometric mean of the two corner frequencies. Thus the aim is to design the speed controller such that the system gain

crosses the 0 dB point at this frequency, with a slope of -20dB/decade.

Thus choosing  $f_{bw}$  is chosen appropriately,

$$\text{by } f_{bw}^2 = f_w f_{is}$$

condition for  $f_{bw}$  to be gain crossover frequency of the loop be give as

$$\frac{K_p K_{t_{mr}}^* (1+sT_w)}{J t_w s^2 (1+sT_{is})} = 1; @s=2\pi f_{bw}$$

since  $T_w \gg T_{bw}$  and  $T_{is} \ll T_{bw}$  approximating and simplifying

gives

$$K_p = \frac{2\pi f_{bw} J}{K_{t_{mr}}^*}$$

$$\text{and } K_i = \frac{K_p}{T_w}.$$

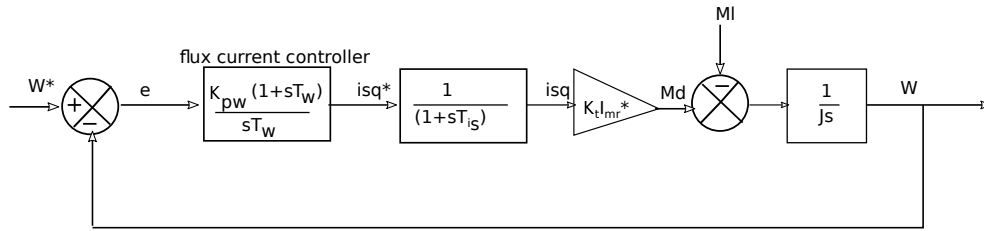


Figure 2.9: Speed controller loop.

### Calculation of limiter values of controllers:

For given 30KW Induction machine

Rated speed of rotor flux = 314 elect.rad/sec.

rated speed of motor = 303.68 elect.rad/sec.

rated Torque = 197.57Nm.

also,

$$T_r = \frac{L_r}{R_r} = 0.366s,$$

$$\sigma_r = \frac{L_{lr}}{L_m} = 0.0297,$$

$$\sigma = \frac{L_s L_r - L_m^2}{L_r L_s} = 0.0567$$

$$\text{and } i_{sq} = \sqrt{\frac{(W_m R - W) M_d T_r}{K_t}} = 117.92 A$$

$$K_t = \frac{2}{3} \frac{P}{2} \frac{L_m}{1 + \sigma_r} = 0.05855 \text{ Nm/A}^2$$

$$i_{sd} = \frac{M_d}{0.0588 i_{sq}} = 30.7821 \text{ A}$$

The rated value of  $i_{mr}$  is same as  $i_{sd}$  in steady state.

$$V_{sd} = R_s i_{sd} - \sigma L_s W_{mr} i_{sq} = -94.006 \text{ V}$$

$$V_{sq} = R_s i_{sq} + \sigma L_s W_{mr} i_{sd} + (1 - \sigma) L_s W_{mr} i_{mr} = 465.26 \text{ V}$$

## 2.3 Simulation results:

Below are the given results for the 30KW given Induction motor

From the given figure 2.10 we can see that on application of supply voltage the current initially rises to a value around 100 A which is in the permissible limits, without vector control current may rise to 10 to 15 times of the rated value initially which is partially dangerous. finally current can be seen to settle at rated value after around 1.5 seconds for vector control.

figure 2.11 shows Speed profile for Induction motor with vector control with reference value of 1400rpm, Speed curve can be seen to smoothly rise and settle at reference with proper controller constants calculation.

figure 2.12 gives d-axis and q-axis current plots, It is evident that the currents profile are DC which serves the purpose of choosing rotor flux axis as reference axis.

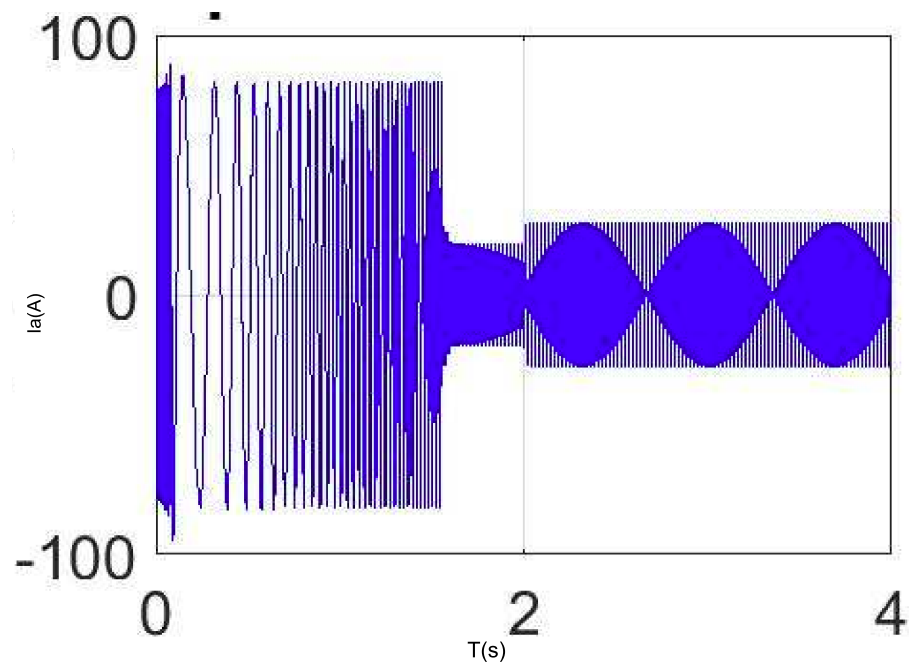


Figure 2.10: Induction motor 3 phase current profile during starting with vector control.(Scale: X-axis 2 sec/div , Y-axis 100A/div)

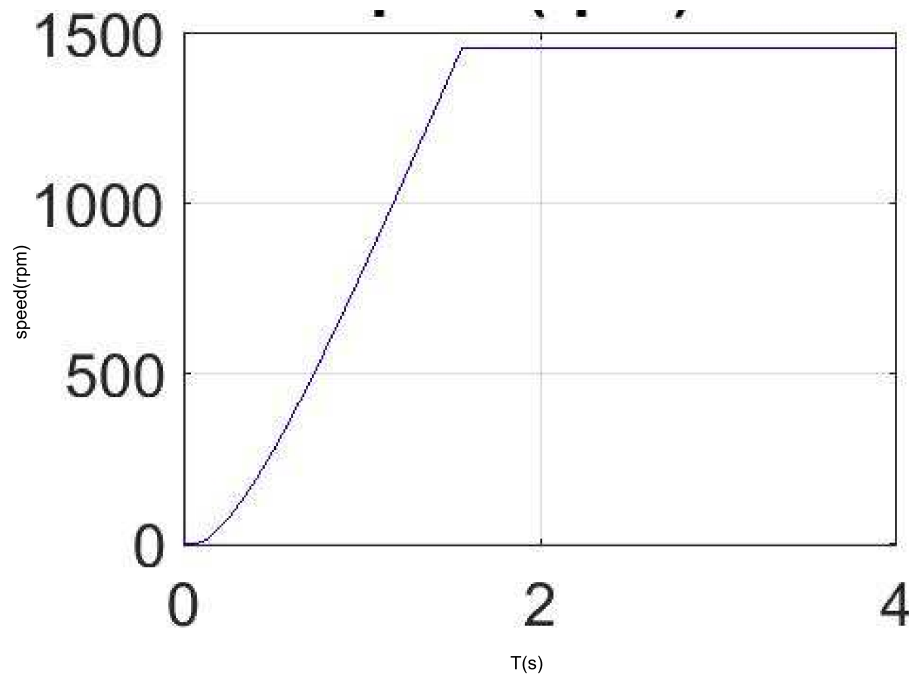


Figure 2.11: Speed response with full load torque being applied from starting.(Scale: X-axis 2 sec/div , Y-axis 500 rad/sec /div)

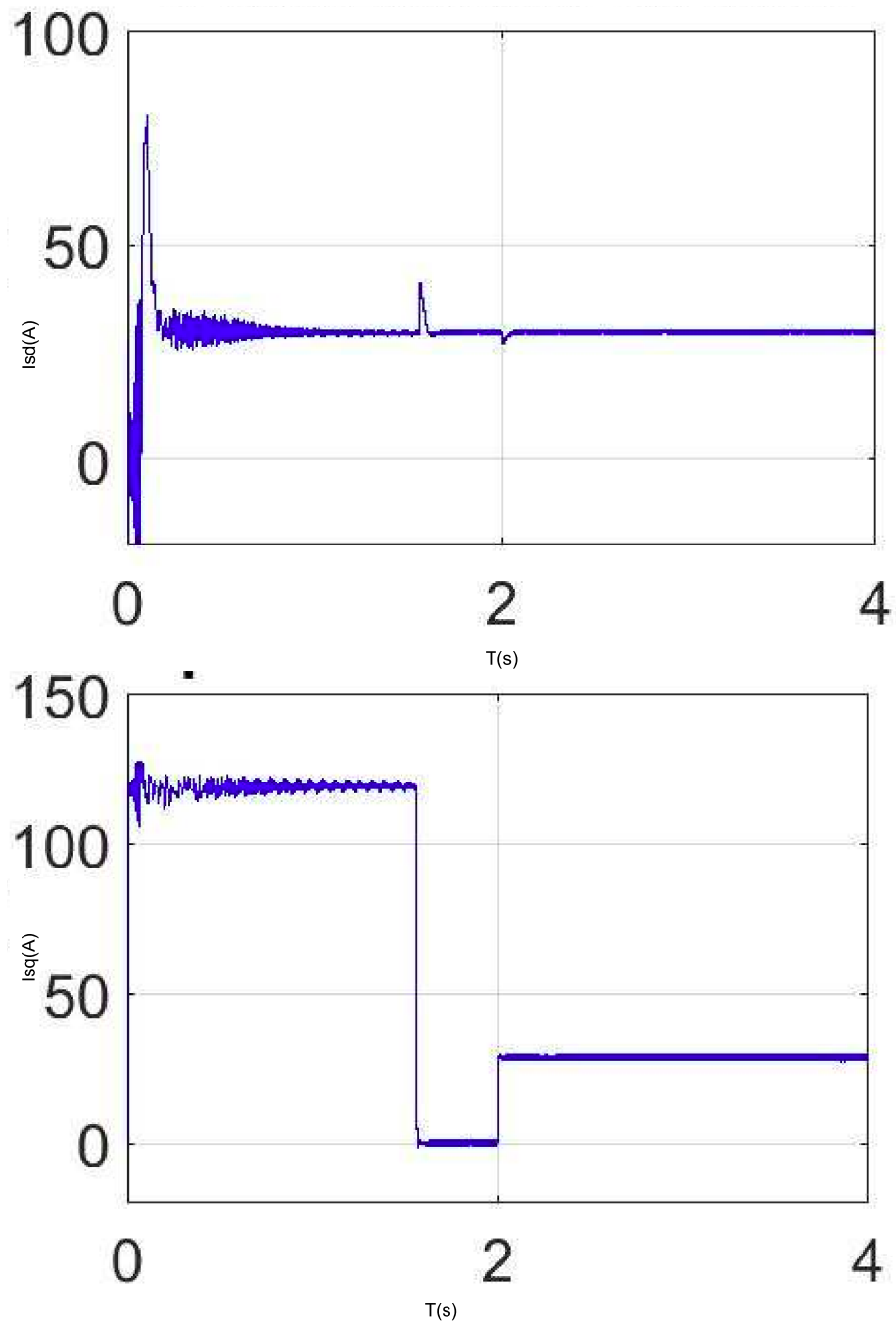


Figure 2.12: d-axis and q-axis current plots for Vector control(Scale: X-axis 2sec/div , Y-axis 50A/div.)



# CHAPTER 3

## Overview of DSP(TMS32028379D)

### 3.1 Introduction

The C28x CPU is a 32-bit fixed-point processor. This device draws from the best features of digital signal processing, reduced instruction set computing (RISC), micro-controller architectures, firmware, and tool sets.

The CPU features include a modified Harvard architecture and circular addressing. The RISC features are single-cycle instruction execution, register-to-register operations, and modified Harvard architecture. The micro-controller features include ease of use through an intuitive instruction set, byte packing and unpacking, and bit manipulation. The modified Harvard architecture of the CPU enables instruction and data fetches to be performed in parallel. The CPU can read instructions and data while it writes data simultaneously to maintain the single-cycle instruction operation across the pipeline. Block diagram for DSP is shown in figure 3.1

In this project we will be using 3 major modules of DSP

1. ePWM
2. ADC & DAC
3. ECAP

for implementing control strategy and modeling of Machine inside DSP.

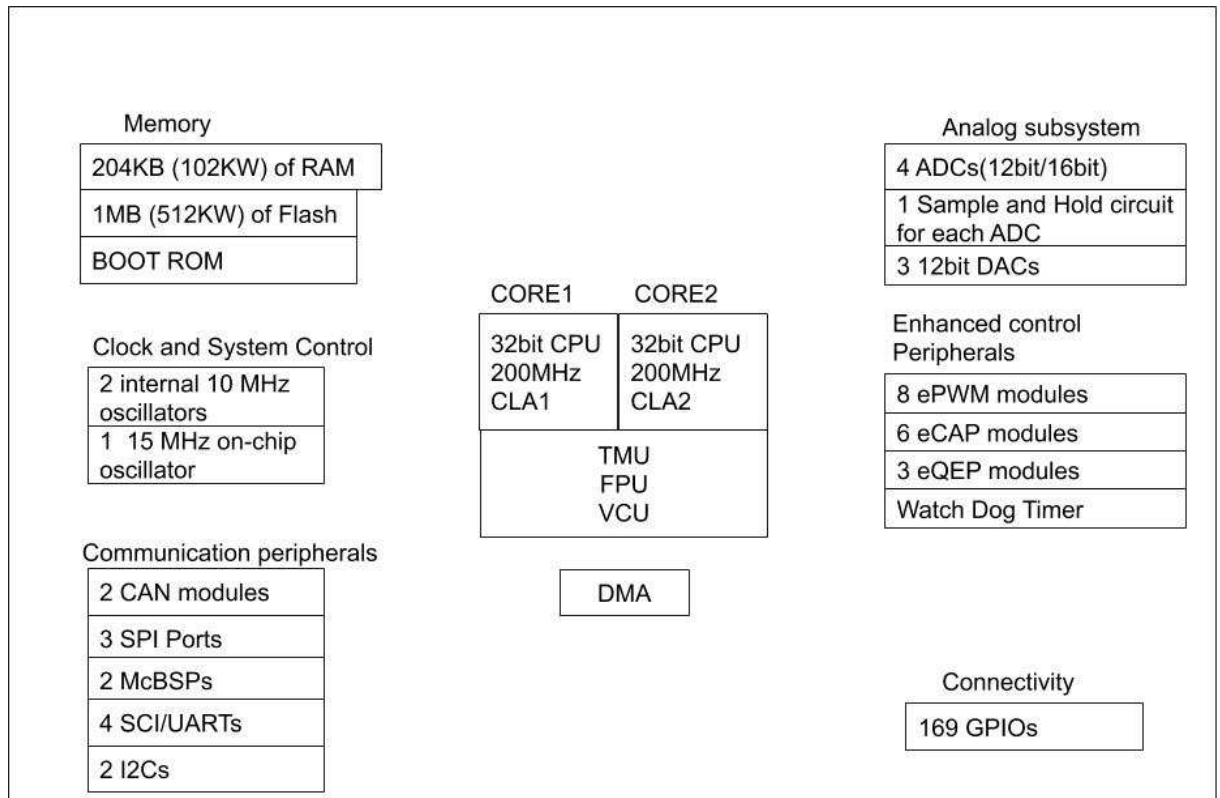


Figure 3.1: Block diagram showing basic features available in TMS320F28379D DSP

## 3.2 ePWM Module:

The enhanced pulse width modulator (ePWM) peripheral is a key element in controlling many of the power electronic systems found in both commercial and industrial equipment. These systems include digital motor control, switch mode power supply control, uninterruptible power supplies (UPS), and other forms of power conversion. The ePWM peripheral can also perform a digital to analog (DAC) function, where the duty cycle is equivalent to a DAC analog value; it is sometimes referred to as a power DAC.

It has 8 ePWM modules which can work individually. Each module has 2 output channels ePWMxA and ePWMxB and each module has 7 sub-modules that can give you various features to trim the output according to your need.

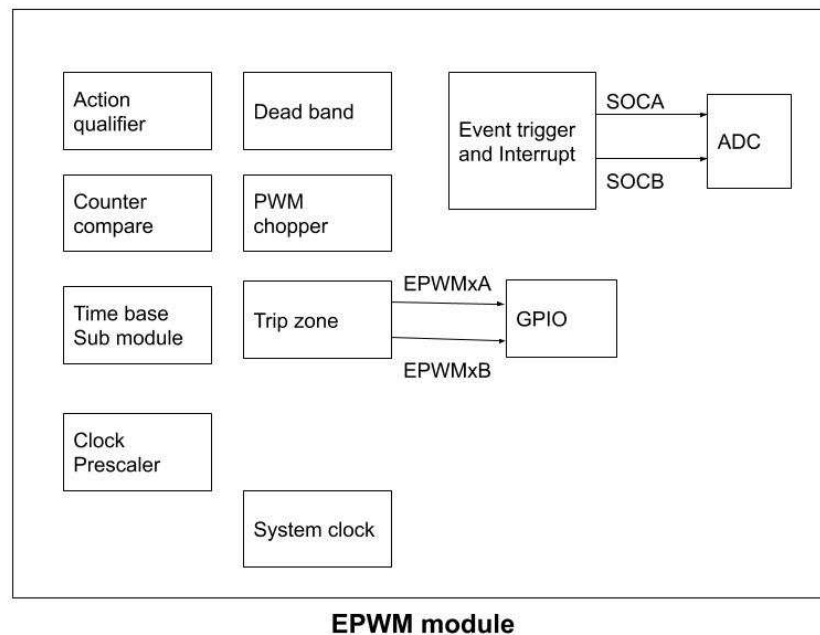


Figure 3.2: Block diagram showing features of EPWM module.

### 3.2.1 TimeBase Submodule

Each ePWM module has its own time-base submodule that determines all of the event timing for the ePWM module. Built-in synchronization logic allows the time-base of multiple ePWM modules to work together as a single system.

Time base submodule can be configured in various ways .It has a separate counter called Time base counter (TBCTR) which keeps the track of system ,it starts counting itself as soon as the Epwm module is enabled and keeps on counting to a certain value called TBPRD(time base period register).For timing synchronizing of a particular event values of TBPRD and TBCTR plays an major role.

Time base submodule can be made to count in 3 modes i.e up-count,down-count,up-and-down count mode.Basically these modes represent counting of TBCTR values.

We can also set TBCTR counts rate by prescaling the ePWM clock.which will allow the time-base counter to increment/decrement at a desired rate.

### 3.2.2 Counter-Compare Submodule

The counter-compare submodule takes as input the time-base counter value. This value is continuously compared to the counter-compare A (CMPA) counter-compare B (CMPB) counter-compare C (CMPC) and counter-compare D (CMPD) registers. When the time-base counter is equal to one of the compare registers, the counter-compare unit generates an appropriate event.

The counter compare module generated events based on programmable time stamps using CMPA,CMPB,CMPC,CMPD registers,In control algorithms it is very useful when we need changes in duty cycle,thus these duty cycle changes can be easily obtained by varying counter compare register values.

Depending on the mode selected(up,down,up-down) in time base sub-module number of counter compare values occurring in a period varies and hence the procedure to get duty cycle has to be managed carefully.

### 3.2.3 Action Qualifier Sub-module

The action-qualifier submodule has the most important role in waveform construction and PWM generation. It decides which events are converted into various action types, thereby producing the required switched waveforms at the EPWMxA and EPWMxB outputs.

Action qualifier sub-module is responsible for generating actions based on the events occurred,

as discussed earlier we have compare registers,which can be given values by the user we can set their values to match with TBCTR at certain point and as soon as the values of both TBCTR and compare register values matches an event is generated .(TBCTR matching with TBPRD or zero value is also an event)

At such a event we can define certain tasks to be carried out by DSP which can be done by action qualifier sub-module.We can also independently give tasks in up-down mode where events can occur twice per period.

i.e one event occurs at TBCTR is increasing and another occurs when TBCTR is

decrementing.

### **3.2.4 Dead Band Generator Sub-module**

The action-qualifier (AQ) module section discussed how it is possible to generate the required dead band by having full control over edge placement using both the CMPA and CMPB resources of the ePWM module. However, if the more classical edge delay-based dead band with polarity control is required, then the dead-band sub-module described here should be used.

Dead band submodule generated appropriate signal pairs (EPWMxA and EPWMxB) with dead-band relationship for a single EPWMxA input. It has various programmable signal pairs which can be used to modify the basic EPWM outputs. or if not required it can be bypassed.

Deadband plays an important role in controlling of circuitry with complimentary switching .wherein certain delay has to be given between turning off and turning on of switches for safety of circuit.

### **3.2.5 Event Trigger Sub-module**

The event-trigger sub-module manages the events generated by the time-base sub-module, the counter- compare sub-module, and the digital-compare sub-module to generate an interrupt to the CPU and/or a start of conversion pulse to the ADC when a selected event occurs.

Event trigger sub-module receives input from time-base, counter-compare and digital compare sub-modules.

Based on the personal requirements it can be used to prescale logic to issue interrupt requests and ADC start of conversion signals at every event, every second event and up to every fifteenth event.

It has dedicated registers to provide full visibility of event generation via event counters and flag registers, i.e if an certain event has occur it will increment count to counter to +1 and flag will be given certain value to show that and particular event has occurred

or completed.

Also event trigger submodule can be used for software forcing of interrupts and ADC start of conversion.

### 3.3 ADC Module

The ADC module is a successive approximation (SAR) style ADC with Preferable resolution of either 16 bits or 12 bits. The ADC is composed of a core and a wrapper. The core is composed of the analog circuits which include the channel select MUX, the sample-and-hold (S/H) circuit, the successive approximation circuits, voltage reference circuits, and other analog support circuits. The wrapper is composed of the digital circuits that configure and control the ADC. These circuits include the logic for programmable conversions, result registers, interfaces to analog circuits, interfaces to the peripheral buses, post-processing circuits, and interfaces to other on-chip modules. Each ADC module consists of a single sample-and-hold (S/H) circuit. The ADC module is designed to be duplicated multiple times on the same chip, allowing simultaneous sampling or independent operation of multiple ADCs.

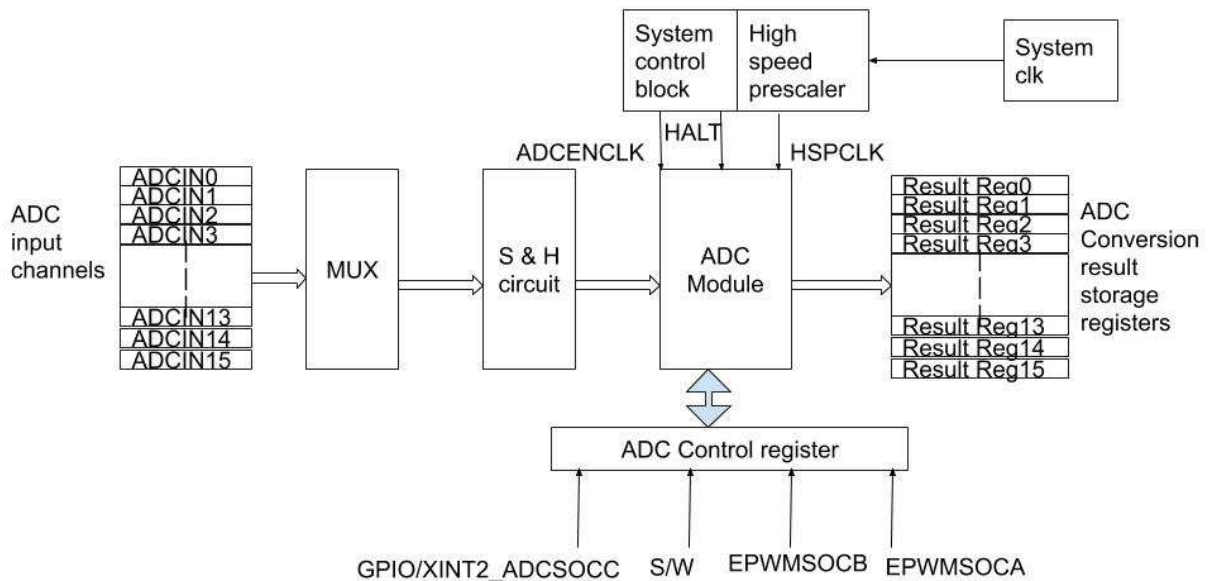


Figure 3.3: Block diagram showing ADC module.

### **3.4 DAC Module:**

The buffered DAC module consists of an internal 12-bit DAC and an analog output buffer that is capable of driving an external load. An integrated pull-down resistor on the DAC output helps to provide a known pin voltage when the output buffer is disabled. This pull-down resistor cannot be disabled and remains as a passive component on the pin, even for other shared pin-mux functions. The buffered DAC is a general-purpose DAC that can be used to generate a DC voltage in addition to AC waveforms such as sine waves, square waves, triangle waves and so forth. Software writes to the DAC value register can take effect immediately or can be synchronized with EPWMSYNCPER events.

### **3.5 eCAP Module:**

The eCAP module allows time based logging of external logic signal transition on pins, Thus it can be used to measure speed by measuring the time interval between the pulses from one channel of the encoder. The basic block diagram of capture module on given DSP is shown. Each capture unit is associated with a capture pin and an event prescaler that reduces the input signal frequency. Polarity select bit fields can be used to configure rising or falling edge as the trigger. The system clock increments a 32-bit time stamp counter. When a trigger occurs, the current value of the counter is saved in the capture register and the counter is reset. Then this value is used in speed calculation.

It can also be used as resource to generate single channel PWM generator.

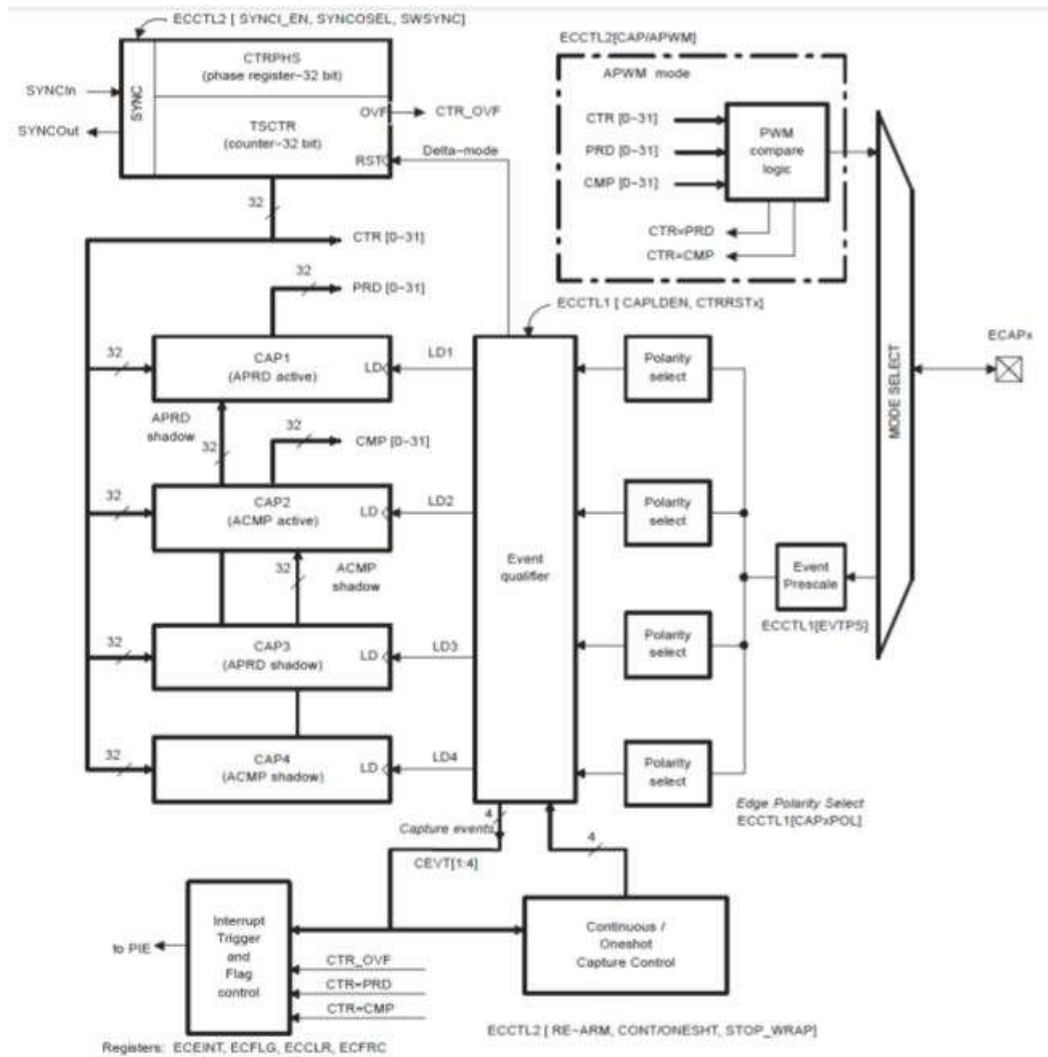


Figure 3.4: eCAP Module Reference-Technical reference module TI, literature no.SPRUHM8I, December-2013-Revised September 2019.



# CHAPTER 4

## DSP simulations

### 4.1 R-L simulation in DSP

In this section a basic R-L load circuit was implemented in DSP with the value of  $R=1\Omega$  and  $L = 1\text{mH}$ , having supply voltage of  $100\text{v}, 50\text{hz}$ . We will verify the DSP results with the analytically calculated solution, which is given below.

#### 4.1.1 Analytical solution:

$$V = Ri + L \frac{di}{dt} \quad (4.1)$$

$$i = \int \frac{V - Ri}{L} dt \quad (4.2)$$

Hence we can say that 'i' waveform should be phase lagging by an angle of  $\tan^{-1}\left(\frac{2\pi fL}{R}\right)$  and should have a peak of magnitude 95.40 after integration. with the above given circuit values.

#### 4.1.2 Implementation in DSP

Since DSP works in discrete domain we need to break the equation(4.1) in time digital form to evaluate by samples.

Therefore numerical methods can be implemented for step by step calculation.

Here Runge-Kutta 4th order method is used based on the fact that it is easy to implement and very stable .

According to Runge - Kutta method :

$$k_1 = hf(X_n, Y_n) \quad (4.3)$$

$$k_2 = hf(X_n + 0.5h, Y_n + 0.5k_1) \quad (4.4)$$

$$k_3 = hf(X_n + 0.5h, Y_n + 0.5k_2) \quad (4.5)$$

$$k_3 = hf(X_n + h, Y_n + k_3) \quad (4.6)$$

Therefore,

$$Y_{n+1} = Y_n + 0.16(K_1 + 2K_2 + 2K_3 + K_4) \quad (4.7)$$

this equation has to be solved in a loop unless  $Y_{k+1} = Y_k$  is obtained ideally.

where  $(K+1)^{th}$  term is next approximate term

$K^{th}$  term is Present term.

hence, for our model starting from the initial guess of  $X_n(i)$ ,  $Y_n(v) = 0$ .

calculate constants  $k_1, K_2, K_3, K_4$

and get

$$i_{K+1} = i_k + 0.16(K_1 + 2K_2 + 2K_3 + K_4) \quad (4.8)$$

has to be implemented with suitable loop time of  $h$  so as to get convergent solution i.e the present value of the variable should match next approximate value ideally . here we have used  $h=40\mu\text{sec}$ , based DSP control constraints and suitability of equations. From the waveform shown in figure 4.1 it is evident that both the signals are 15.75 degree phase shifted, with a current signal having magnitude of 95.5A. With given parameters of supply voltage 100v, 50hz,  $R=1\Omega$ ,  $L=1\text{mH}$ .

The above given method to implement a single differential equation can be further expanded to multiple differential equations which we have used in the next section to model an Induction motor with the help of equations derived in section 2.2.4.

Figure 4.1 confirms the result and it can be seen that the analytical calculation and DSP calculations matches validating the method used.

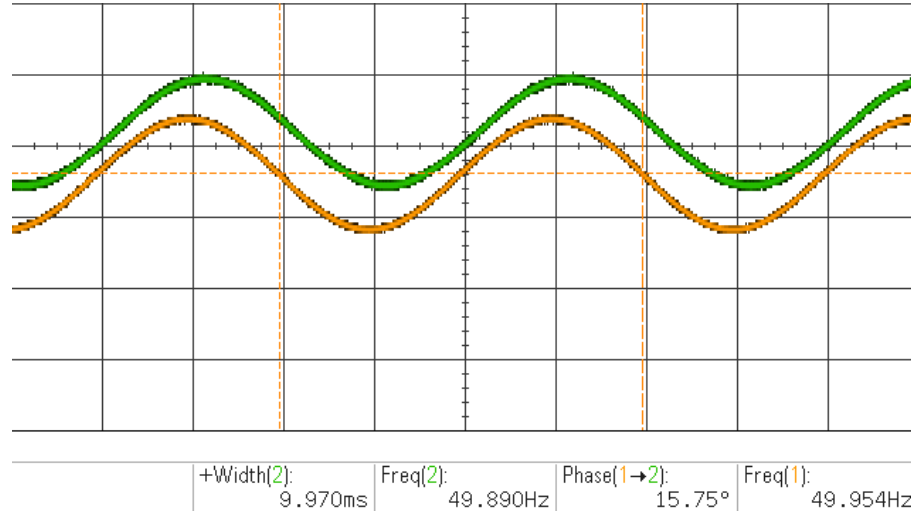


Figure 4.1: RL load simulated in DSP with Orange line as voltage signal and green line as current signal. ( Scale: X-axis 2sec/div , Y-axis 20units/div.)

## 4.2 Online Modeling of Induction motor

Online modeling Induction motor refers to modeling of a motor in any such platform where it can be tested directly on the go. Here we have used TMS320F28379D DSP Platform by Texas Instruments for modeling of motor.

The model based design approach is a very convenient method it helps you in continuously verifying and validating every basic steps involved in designing, which imparts inherent robustness to the system against any coding errors related to control algorithm. The model-based design is significantly different from traditional design methodology. Rather than using complex structures and extensive software codes, designers can use Model-based design to define plant models with advanced functional characteristics using continuous-time and discrete-time building blocks. These built models used with simulation tools can lead to rapid prototyping, software testing, and verification. Not only is the testing and verification process enhanced, but also, in some cases, hardware-in-the-loop simulation can be used with the new design paradigm to perform testing of dynamic effects on the system more quickly and much more efficiently than with traditional design methodology.

.Since we have already discussed all the basic building blocks required in Chapter 3 DSP learning ,In section 4.1 and 4.2 we will focus on using them. Equations regarding modeling(30KW motor) were earlier derived in section 2.2.4. and are used here in

modeling.

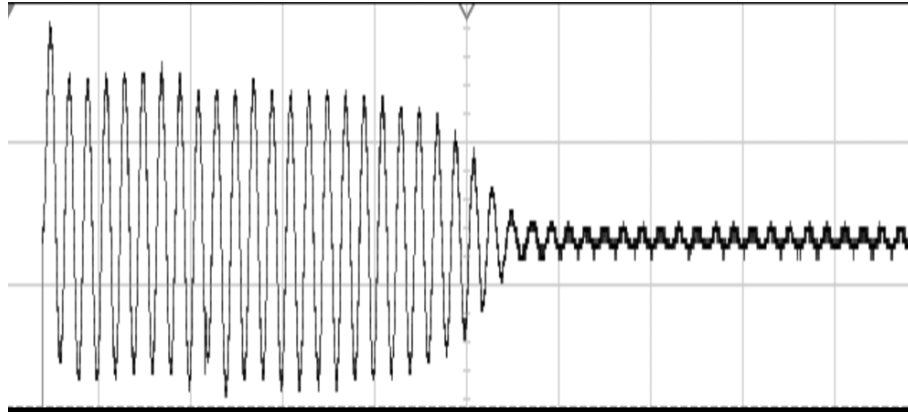


Figure 4.2: a phase Rotor current profile for Induction motor at no load. ( Scale: X-axis 5msec/div , Y-axis 500 units/div.)

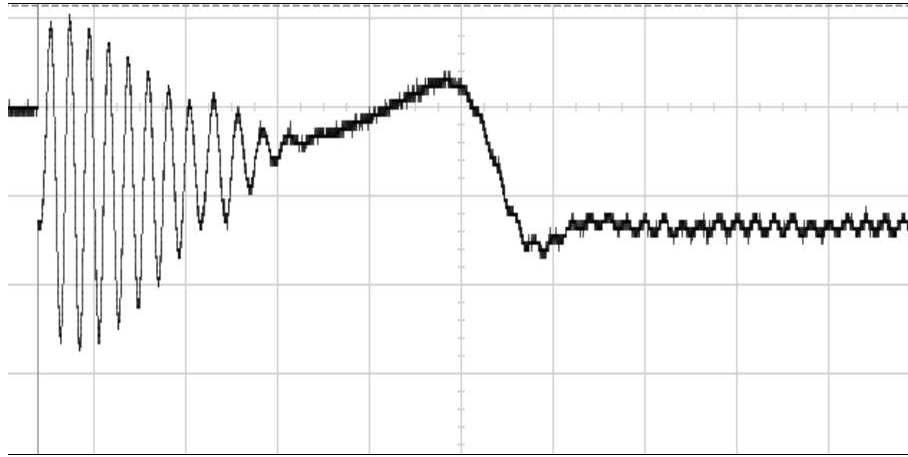


Figure 4.3: shows Torque profile for Induction motor at no load. ( Scale: X-axis 5msec/div , Y-axis 500rpm/div.)at no load

figure 4.3 shows torque and figure 4.2 shows current profile for Induction motor when load is not applied. We can see that the current rises to dangerously high value which is approximately 6-8 times the current with respect to the settled value of current. and generated torque value can be seen to settle almost zero which is not load condition. Hence in order to restrict current a suitable control algorithm has to be implemented for better control and protection.

Figure 4.4 shows d-q axis currents  $I_{sd}$ ,  $I_{sq}$  current profiles which can be seen to be fairly constant values serving the purpose of converting AC values to a DC for facilitating faster and easy control.

figure 4.5 shows sine of  $\rho_{mr}$  which is almost 180 degrees phase shifted with sine of

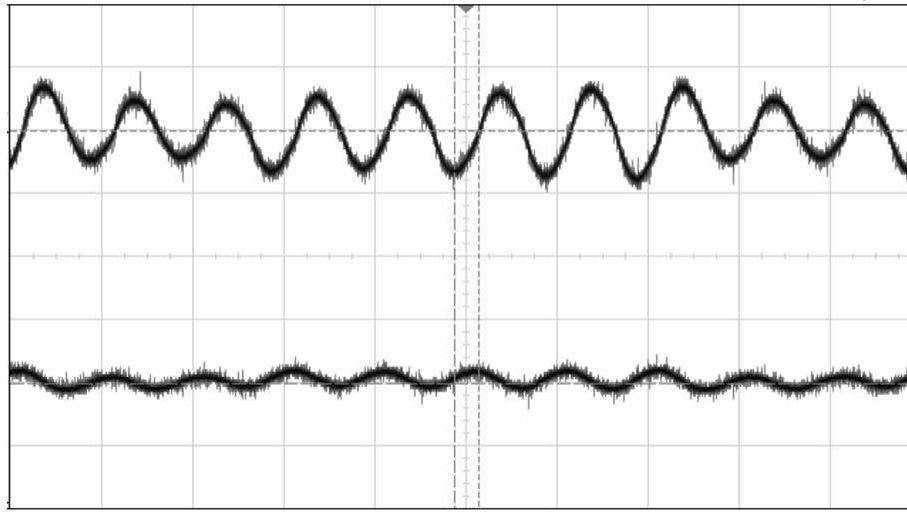


Figure 4.4: d-axis and q-axis profiles for dq reference currents. Upper one represents  $I_{sd}$ , lower one represents  $I_{sq}$  ( Scale: X-axis 5msec/div , Y-axis 500mv/div.)

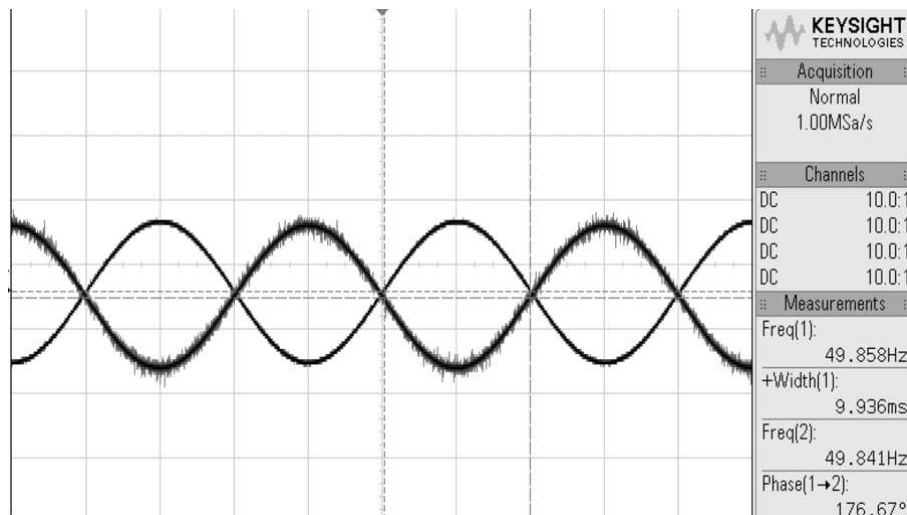


Figure 4.5:  $\sin(\rho_{omr})$  plot vs supply sine wave. ( Scale: X-axis 5msec/div , Y-axis 1 unit/div.)

supply signal and having frequency of 50hz indicating rotor flux rotates at synchronous speed. Although phase angle with supply sine signal will vary with change load.

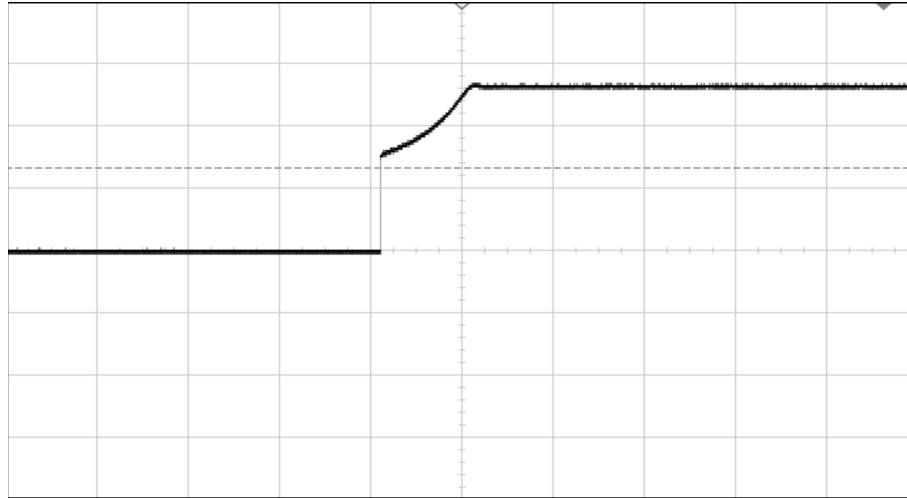


Figure 4.6: Rotor speed profile for Induction motor when a load of ( Scale: X-axis 5msec/div , Y-axis 500units/div.)

Figure 4.6 shows speed profile for Rotor of Induction motor which can be seen to rise smoothly to a value of approximately 1490rpm at no load. Speed settling will depend on the amount of load torque applied . at rated value of torque the speed will be 1450rpm. Hence to make the motor useful for required application suitable control strategy has to be applied to vary speed.

### 4.3 V/f applied to Induction motor.

The Focus of V/f control of Induction motor is to keep the ratio of supply voltage to supply frequency constant through out the process so as to keep the air gap flux inside machine to a constant value. In this method we will generate a constant ramp signal linking both flux and voltage vectors with it, In practice the stator supply voltage to frequency ratio is usually based on the rated values of these variables. as shown in figure 4.8 below

from figure 4.8 it is evident that initially the signal magnitude is less and rising continuously with increasing frequency indicated by thickening in signal lines keeping v/f ratio constant until their rated values are reached.

Initially on application of supply voltage the profile of voltage vs frequency will not

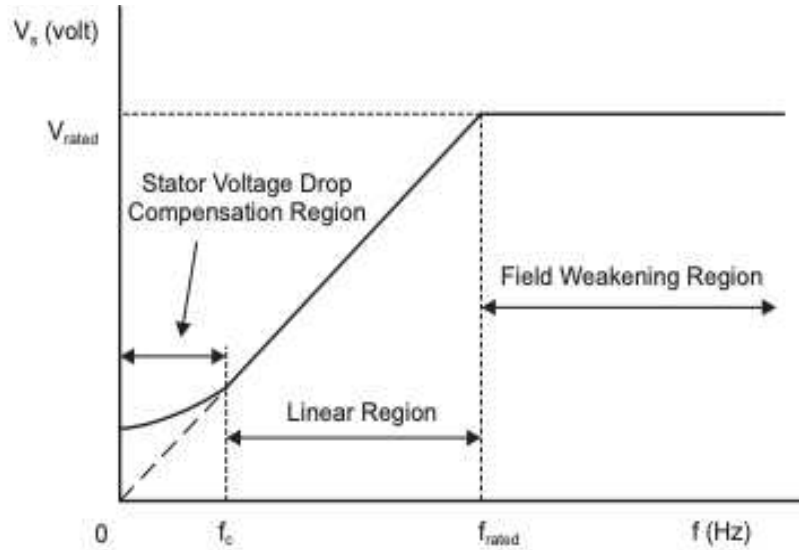


Figure 4.7: Strategy to implement V/F method

be linear since there will be stator resistance drop. Hence a cutoff frequency  $f_c$  and a suitable stator voltage has to be calculated from equivalent circuit of Induction motor with  $R_s(\text{stator resistance}) \neq 0$ ,

Similarly  $v/f$  ratio cannot be satisfied at higher than rated voltage due to insulation breakdown constraints. Therefore, the resulting air gap flux would be reduced, and this will unavoidably cause the decreasing developed torque correspondingly. This region is usually so called “field-weakening region”. To avoid this, constant  $V/\text{Hz}$  principle is also violated at such frequencies. Concluding we should always operate in "Linear Region" for  $v/f$  control. Below given figure 4.9 shows the DSP waveform generated  $v/f$  waveform.

Since now we have made  $v/f$  ratio constant through out. The air gap flux inside the motor is constant irrespective of change in frequency. Hence motor torque will only depend on slip speed, Therefore By regulating the slip speed, the torque and speed of an Induction motor can be controlled with the constant  $V/f$  principle. Here  $v/f$  supply is given to a Induction motor with following ratings:

figure 4.10 shows the current profile for  $v/f$  supply, We can see that the current magnitude is slowly increasing due to  $v/f$  supply which was one of the idea behind application of control. Finally current will settle to a value corresponding to applied load torque. Here we have applied 50Nm of load torque the current was seen to be settling at around 60A.

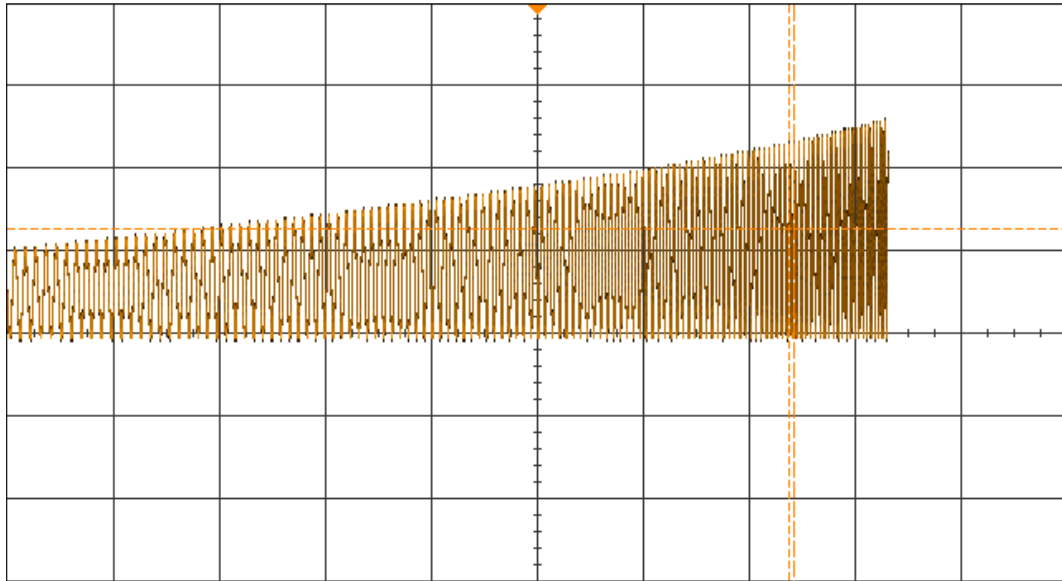


Figure 4.8: V/f generated signal shown in Oscilloscope ( Scale: X-axis 2sec/div , Y-axis 5v/div.)

Parameter	Value
Power	30KW
Voltage	380V
Current	59A
speed	1450rpm
Pf	0.88
Rotor type	Squirrel cage

Figure 4.9: Induction motor rating.

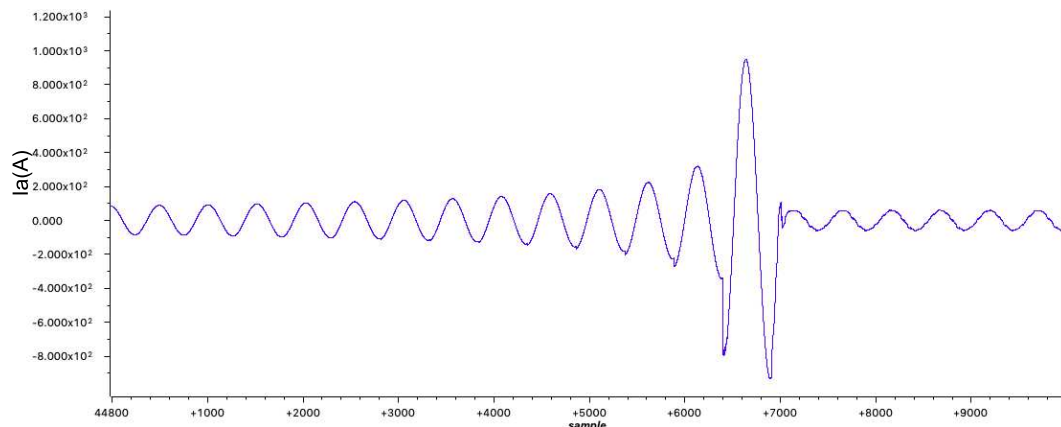


Figure 4.10: Current profile when V/f supply is applied at 50Nm load.(Scale:Y-axis current in A,X-axis number of samples)



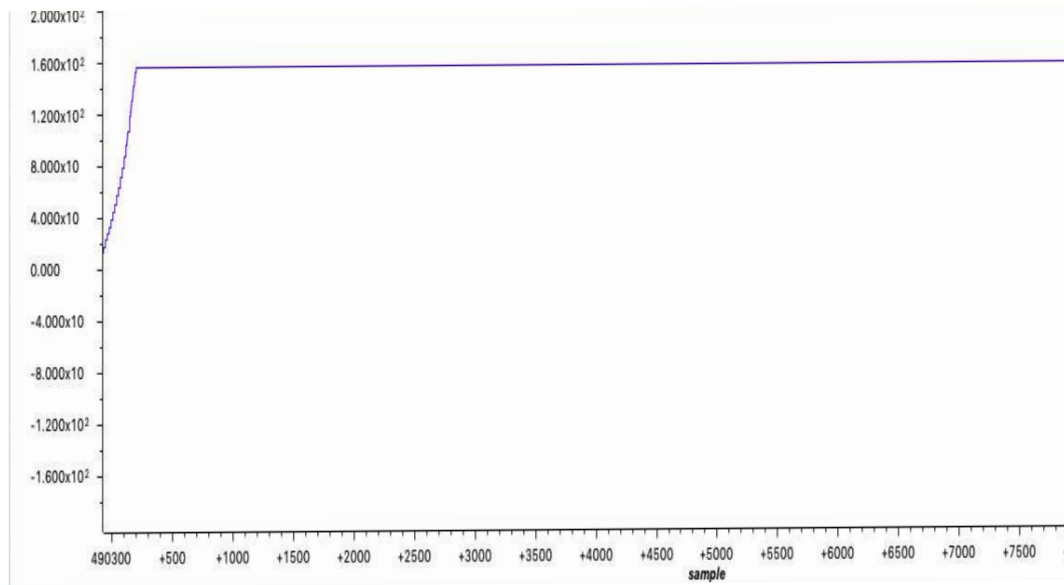


Figure 4.11: Rotor speed with v/f supply at 50Nm load.(Scale: X-axis number of samples,Y-axis speed in rpm)

figure 4.12 shows Rotor Speed profile for Induction motor with applied load torque of 50Nm ,Speed profile can be seen to settling at around 1490rpm which is due to rated v/f ratio is given,In v/f control only speed less than rated value can be obtained. Hence to obtain speed less than this we can vary frequency of the supply correspondingly supply voltage and hence the ratio.

## 4.4 Vector control implementation

### 4.4.1 Per unitized model for IM(30KW)

Voltage(Vb)	300V
Current(Ib)	50A
Angular speed(Wb)	314 rad/sec

Figure 4.12: Base values used for per unitization

Since control algorithm implementation can be very complex and tedious process,Per unitization can assist in easing the difficulty.Going by this method all the

quantities are scaled down by using base quantities. So that complex calculations and keeping track of all the values becomes easy and control algorithm can be implemented with ease comparatively. The base values used for per unitization are chosen keeping in mind the maximum quantities are scaled down to a range, where all the variables are confined and comparable to each other. below given are the perunitized motor modeling equation :

$$\frac{dI_{sd}}{dt} = \frac{V_{sd} * V_b}{\sigma * L_s * I_b} - \frac{R_s * I_{sd}}{\sigma * L_s} + \omega_{mr} * W_b * I_{sq} - \frac{1 - \sigma}{\sigma} * \frac{dI_{mr}}{dt} \quad (4.9)$$

$$\frac{dI_{sq}}{dt} = \frac{V_{sq} * V_b}{\sigma * L_s * I_b} - \frac{R_s * I_{sq}}{\sigma * L_s} + \omega_{mr} * W_b * I_{sq} - \frac{1 - \sigma}{\sigma} * W_b * \omega_{mr} * I_{mr} \quad (4.10)$$

$$\frac{dI_{mr}}{dt} = \frac{I_{sd} - I_{mr}}{T_r} \quad (4.11)$$

$$\frac{d\omega_r}{dt} = \frac{M_d - M_l}{J} * \left( \frac{M_b}{W_b} \right) \quad (4.12)$$

$$\frac{d\rho_{mr}}{dt} = \omega_{mr} * W_b. \quad (4.13)$$

Where,

$$\omega_{mr} = \omega_r * \frac{P}{2} + \omega_{slip} \quad (4.14)$$

$$\omega_{slip} = \frac{I_{sq}}{T_r * I_{mr} * W_b} \quad (4.15)$$

#### 4.4.2 controller constants in per unit

$$V_{phasemax} = 537.40v,$$

$$I_{phasemax} = 60A,$$

$$P_W = 30000W,$$

$$J = 1.631Kg.m^2,$$

$$\omega = 2 * \pi * f = 314rad,$$

$$V_{dc} = 800v.$$

$$T_s = 0.000040sec.$$

$$\sigma = 0.0571.$$

Controller constants are calculated as per the guidelines given in section 2.5 of the report and are tabulated below.

Controller	Fb(Hz)	Kp(pu)	Ki(pu)	Umax(pu)	Umin(pu)
Isd	100	0.1815	0.00191	0.410	-0.410
Isq	100	0.1815	0.00191	1.572	-1.572
Imr	10	2.73	0.0001	0.136	-0.136
Wr	5	28.40	0.000089	0.674	-0.674

Figure 4.13: controller constants

In table shown in figure 4.13 given are the PI controller constants to be used for the implementation of vector control of 30Kw induction motor for the given base values. Maximum and minimum values for the controller are calculated considering safety margin of 1.5 times the rated value.

#### 4.4.3 Flux angle estimation

In figure 4.14 shows is the blocked scheme to be implemented in order to obtain the flux angle from motor,since we can access only 4 parameters from machine naming them are 3 phase currents Ia,Ib,Ic and the rotor speed. This estimated flux angle will be further used to calculated d-q axis currents and will acts as feedback to controller. While implementing this scheme RK-4 method was used considering stability and accuracy .

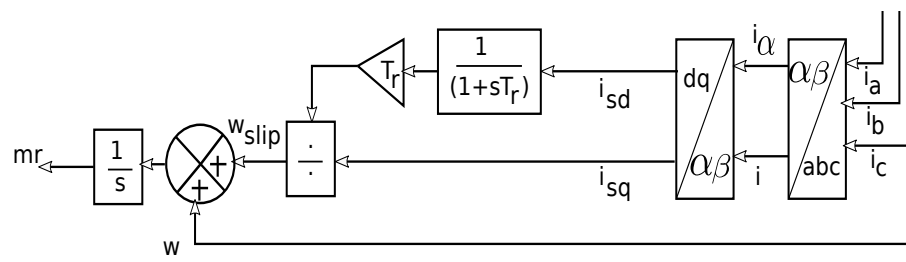


Figure 4.14: FLux angle estimation

# CHAPTER 5

## Conclusion

### 5.1 Summary of work

Simulations for speed separately excited Dc motor, Vector control of Induction motor MATLAB Simulink platform. DSP simulations on TMS320F283789D by Texas Instruments were carried out which included RL load implementation which helped in implementing Induction motor model. Further Online modeling of machine is an important aspect of study which imparts robustness to the control system being implemented and gives prior knowledge about the working condition of system. Then V/f supply was given to the Induction motor and the results were verified with respect to the expected outcomes, They were found in close correspondence. Also an attempt was made to implement vector control algorithm in TMS32028379D with online modeled motor.

### 5.2 Future scope

There remains a wider scope of improvement in present work ,Since the given DSP TMS320F28379D is Dual core and fast processing. We can implement Control part on one processor and Motor model on one processor to make the system faster operating, Since with our work only 20 percent of processor was utilized we can make it work more efficiently with full capacity implementing more complex codes and highly efficient control techniques. Also handling of number of motors can be made possible with at a given instant of time with single control system.

## REFERENCES

- [1] D. Novotny and T. Lipo, Vector Control and Dynamics of AC Drives. Oxford, U.K.: Oxford Univ. Press, 1996.
- [2] Leonhard, Werner, (1985). Control of electrical drives Electrical engineering Electric energy systems and engineering series Research and development. The university of Michigan, Springer-Verlag, 1996.
- [3] Jose Titus, Sensored and sensorless field oriented control for an Induction motor drive, Project report for Master of technology, IIT Madras May 2014.
- [4] P.C Krause and S. Steudloff, Analysis of Electric Machinery, IEE 2001.
- [5] C2000™ MCU 1-Day Workshop Workshop Guide and Lab Manual by Texas Instruments, C2000 MCU 1-Day Workshop Revision 2.0 November 2016
- [6] TMS320F2837xD Dual-Core Microcontrollers Technical Reference Manual, Literature Number: SPRUHM8H December 2013 – Revised January 2019.
- [7] Lori Heustess, Texas Instruments .Programming TMS320x28xx and 28xx Peripherals in C, C++. Texas Instruments Application Note, Literature Number : SPRAA85D, Jan 2013.
- [8] TMS320C64x+ IQmath Library User's Guide by Texas Instruments. Literature Number: SPRUGG9 December 2008